ARTICLE IN PRESS

International Journal of Forecasting xxx (xxxx) xxx

Contents lists available at ScienceDirect

International Journal of Forecasting

journal homepage: www.elsevier.com/locate/ijforecast

Wind energy forecasting with missing values within a fully conditional specification framework

Honglin Wen[a,c,*], Pierre Pinson[b,c,**], Jie Gu[a], Zhijian Jin[a]

[a] *Department of Electrical Engineering, Shanghai Jiao Tong University, China*
[b] *Dyson School of Design Engineering, Imperial College London, United Kingdom*
[c] *Department of Technology, Management and Economics, Technical University of Denmark, Denmark*

ARTICLE INFO

Keywords:
Wind power
Probabilistic forecasting
Missing values
Multiple imputation

ABSTRACT

Wind power forecasting is essential to power system operation and electricity markets. As abundant data became available thanks to the deployment of measurement infrastructures and the democratization of meteorological modeling, extensive data-driven approaches have been developed within both point and probabilistic forecasting frameworks. These models usually assume that the dataset at hand is complete and overlook missing value issues that often occur in practice. In contrast to that common approach, we here rigorously consider the wind power forecasting problem in the presence of missing values, by jointly accommodating imputation and forecasting tasks. Our approach can infer the joint distribution of input features and target variables at the model estimation stage based on incomplete observations only. We place emphasis on a fully conditional specification method, owing to its desirable properties, e.g., being assumption-free when it comes to these joint distributions. Then, at the operational forecasting stage, with available features at hand, one can issue forecasts by implicitly imputing all missing entries. The approach is applicable to both point and probabilistic forecasting, while yielding competitive forecast quality in both simulated and real-world case studies. The results confirm that by using a powerful universal imputation method based on a fully conditional specification, the proposed universal imputation approach is superior to the common impute-then-predict approach, especially in the context of probabilistic forecasting.

1. Introduction

1.1. Background

As a cornerstone to achieve net-zero emissions in the energy sector, wind power has proliferated over recent decades. However, the stochastic nature of wind power generation challenges power system operation and electricity markets, thus motivating wind power forecasting (WPF) research. WPF is usually classified into short-term forecasting (hours to a few days), which takes numerical weather predictions as input features; and very-short-term forecasting (minutes to a few hours), which utilizes recent observations as input features. Recently WPF has achieved several advances by employing cutting-edge statistical and machine learning approaches, e.g. deep learning (Goodfellow, Bengio, & Courville, 2016) and lightGBM (Ke et al., 2017), and by modeling the underlying stochastic processes through the investigation of their spatiotemporal dynamics (Cavalcante, Bessa, Reis, & Browell, 2017; Messner & Pinson, 2019).

Meanwhile, the interest of the WPF community has shifted from point forecasting to probabilistic forecasting;

[*] Corresponding author at: Department of Electrical Engineering, Shanghai Jiao Tong University, China.
[**] Corresponding author at: Dyson School of Design Engineering, Imperial College London, United Kingdom.
E-mail addresses: linlin00@sjtu.edu.cn (H. Wen), p.pinson@imperial.ac.uk (P. Pinson).

https://doi.org/10.1016/j.ijforecast.2022.12.006
0169-2070/© 2022 International Institute of Forecasters. Published by Elsevier B.V. All rights reserved.

see the recent review by Hong et al. (2020). Probabilistic wind power forecasting (PWPF) communicates the probability distribution of wind power generation at a future time based on gathered information up to the issue time, usually in the form of quantiles, prediction intervals, and densities. It has attracted increasing attention in the power industry, especially after the 2014 Global Energy Forecasting Competition (GEFCom 2014) (Hong et al., 2016). In general, two approaches, namely parametric and non-parametric, have been proposed for PWPF. The parametric approach is based on a distributional assumption, such as Gaussian, beta, etc., the shape parameters of which are determined through statistical learning. In contrast, the non-parametric approach is free of such an assumption. One of the most popular non-parametric approaches relies on quantile regression (QR) (Koenker & Hallock, 2001), which involves a pinball loss function to guide the learning of conditional quantile functions. It is therefore easy to employ QR in advanced statistical learning models (for instance gradient boosting machines (Landry, Erlinger, Patschke, & Varrichio, 2016) and extreme learning machines (Wan, Lin, Wang, Song, & Dong, 2016)) by using the pinball loss as the loss function at the model estimation phase. Besides, with the aim of characterizing the whole distribution in a distribution-free manner, methods that simultaneously estimate several quantiles (Sangnier, Fercoq, & d'Alché Buc, 2016) and directly estimate the distribution based on conditional normalizing flow(s) (Wen, Pinson, Ma, Gu, & Jin, 2022) have been proposed.

Although several works have contributed forecasting methods and products to the WPF community, most of them assume that the dataset at hand is complete, and overlook the widespread missing value problems, due to sensor failures and communication errors, for instance. Intuitively, missing value issues pose problems at both the model estimation and operational forecasting stages, ultimately compromising forecast quality. Obviously, for models estimated through gradient-based optimization, the training datasets cannot contain missing values. Otherwise, the gradients of the parameters cannot be calculated at the model estimation stage. Therefore, rows of the learning set containing both missing values and observations are often deleted, even if the missing information is minimal. This means that valuable information is also discarded in the process of removing the missing values. In addition, even with estimated models at hand, missing value problems still affect operational forecasting, possibly obliging forecasters to revert to naive models such as climatology (i.e., long-term averages) as surrogates. Therefore, it remains an open issue to investigate the influence of missing values and develop WPF approaches that accommodate missing values.

1.2. Related works

An intuitive and popular approach to the problem (though not used by the WPF community) is to impute these missing values before training models and issuing operational forecasts (Liu, Wei, & Zhang, 2018). It is referred to as the "impute-then-predict" (ITP) approach in this paper. For example, the classic forecasting package "forecast" (Hyndman & Khandakar, 2008) provides an option that uses linear interpolation to impute missing values. Obviously, a spectrum of imputation methods can be employed; see the thorough review by Van Buuren (2018). Then, an associated question is how to choose the imputation method. The recent study by Tawn, Browell, and Dinwoodie (2020) suggests that the influence of imputation on model estimation and operational forecasting stages is ambiguous. They concluded that advanced imputation methods are beneficial to model estimation. However, at the operational forecasting stage, it turns out that retraining models without missing features results in better performance. In fact, it is natural to consider the retraining approach, as it only uses actual observations to estimate parameters, and hence prevents using the aforementioned imputation procedure. However, the learning then only relies on a subset of the data available, while the information potentially contained in the discarded part is lost. In addition, this approach may suffer from the curse of dimensionality, since it must train models for all combinations of input features. This may yield a substantial increase in computational costs.

In addition to the aforementioned approaches, several works have focused on adapting forecasting methods to be used in the presence of missing values. A classic approach is based on state-space modeling, where the Kalman filter is modified to accommodate incomplete observations. For example, autoregressive moving average models (Jones, 1980) and autoregressive integrated moving average models (Kohn & Ansley, 1986) have been represented in state-space form and adapted to tackle missing value problems. Although these works have shed light on forecasting in the presence of missing values, they are only applicable to point forecasting and restricted to linear models. Recent advanced models such as GRU-D (Che, Purushotham, Cho, Sontag, & Liu, 2018) and BRITS (Cao et al., 2018) have been proposed based on the long short-term memory model (Hochreiter & Schmidhuber, 1997), by using the intermediate results (which can be also interpreted as latent states) of a neural network model to impute missing values. This idea has been successfully applied in the recent popular package DeepAR (Salinas, Flunkert, Gasthaus, & Januschowski, 2020). However, such models still require imputing missing values via the recurrent neural network structure before performing the forecasting task.

1.3. Proposed method and contributions

There is not a clearly defined boundary between imputation and forecasting, as explained by Golyandina and Osipov (2007). Indeed, a forecasting problem can be considered an imputation problem in a situation where missing values are systematically located at the end of a sequence. Furthermore, both imputation and forecasting tasks assume the continuation of the underlying structure within the data, and consequently leverage observations to predict unknown values. That is, it is feasible to develop a model that can infer the structure based on observations and seamlessly perform the imputation and forecasting tasks. This is referred to as the "universal imputation" (UI) approach in this paper. As a result, in what follows, we use the terms "impute" and "forecast" interchangeably. With this idea in mind, You, Ma, Ding, Kochenderfer, and Leskovec (2020) considered the point forecasting problem and proposed to model the correlation structure between input features and targets via a graph neural network, where imputing missing features and predicting targets can be performed simultaneously. In contrast, we here place ourselves within a probabilistic setting directly, for which it is then also possible to derive point forecasts. Unlike the usual probabilistic forecasting approaches that model conditional probability distributions (for the target variable) directly, in this work, we model the joint multivariate probability distribution of input features and targets. As discussed by Stone (1991), with the estimated multivariate probability distribution at hand, one can obtain conditional distributions via marginalization, although this is computationally inefficient compared to the usual conditional probability distribution modeling. This approach is appealing in the presence of missing values. That is, with the estimated multivariate probability distribution, one can marginalize over missing variables to obtain probabilistic forecasts. Then, the goal at the model estimation stage is to estimate the parameters of such a distribution based on incomplete observations. At the operational forecasting stage, targets to be predicted are treated as missing values and imputed via the estimated distribution. The focus is on very-short-term wind power forecasting applications, where missing value issues often occur, though the method is generic and could be used by others for different applications where accommodating missing values is challenging.

In this work, we focus on situations where observations are missing at random, due to, e.g., sensor failures and communication errors. This means that "missingness" patterns are independent of the missing values themselves. However, it does not mean that this concept of missingness at random is restricted to the case of data missing in a pointwise and sporadic fashion. Even in the case of block missingness (i.e., data missing over time intervals), as long as the data are missing at random (hence, independently of the values for the process of interest or relevant exogenous processes), our approach can be employed. The distribution of missingness can then be left aside when inferring the underlying structure of interest. As a consequence, the problem boils down to estimating the parameters of a model based on incomplete observations only. Cases where missing values are not random could still be handled by the proposed UI approach, though this requires more sophisticated techniques at both the model estimation and operational forecasting stages, something we leave for future work. Specifically, it requires modeling the missingness explicitly when calculating the likelihood at the model estimation stage. At the operational forecasting stage, the targets to be predicted are treated as missing, and thus independent of the missingness distribution of the contextual features. This also requires taking into account the missingness distribution of contextual features when calculating the conditional distribution of missing variables given the observed variables. Particularly, we implement this idea based on the multiple imputation method (Dempster, Laird, & Rubin, 1977), which allows us to impute missing values with several equally likely realizations from the distribution and thus provides probabilistic forecasts for the targets. Instead of assuming a special family of distributions and inferring its parameters, we adopt the fully conditional specification (FCS) approach (Van Buuren, Brand, Groothuis-Oudshoorn, & Rubin, 2006), which implicitly specifies the multivariate distribution as a collection of conditional distributions on a variable-by-variable basis. At the model estimation stage, parameters for each conditional distribution are iteratively estimated through a Gibbs sampling procedure. At the operational forecasting stage, missing values are also iteratively imputed on a variable-by-variable basis.

The proposed method is validated based on a simulation study and real-world case studies with wind power data from the USA. The simulation study is based on synthetic data (for both AR and VAR processes) and Monte Carlo simulations, to illustrate and underline the salient features of our approach. This also allows us to analyze the impact of certain characteristics e.g. the rate of missingness, on the performance of the approach, while remaining in a controlled environment within which the results are due to changes in the design, and not to some spurious effects often observed with real-world data. Real-world data from the USA are used for benchmarking instead, and to investigate various aspects of the applicability of the approach in an operational context, e.g., with a focus on pointwise vs. block missingness, various rates of missingness, univariate and multivariate setups, etc. The results show that the proposed approach is superior to existing ITP approaches. The main contributions of this paper are two-fold. One is the proposal of a universal imputation approach, which is general, though inspired by the problem of wind power forecasting in the presence of missing values. Such a universal imputation approach jointly accommodates imputation and forecasting tasks within the universal multiple imputation framework. By design, this approach allows us to generate both point and probabilistic forecasts. The other contribution is to show its applicability to wind power forecasting with missing values, where different types and rates of missingness are present.

The remaining parts of this paper are organized as follows. Section 2 formulates the problem, and Section 3 describes the proposed approach for forecasting in the presence of missing values. Next, the simulation study to show the applicability of the proposed approach is elaborated in Section 4. Section 5 presents case studies with results and discussion. Section 6 concludes the paper.

Notation: In general, we use uppercase letters to denote random variables and lowercase letters to denote the realizations of these random variables. For instance, Y_1 denotes a random variable and y_1 its realization. A collection of random variables is represented as a tuple, which is bracketed with parentheses, such as (Y_1, Y_2) and $(Y_1, \ldots, Y_{10})$. Boldface lowercase and uppercase letters respectively indicate vectors and matrices. Particularly, we use row and column slices to represent parts of a matrix. For instance, let $\boldsymbol{Z}$ represent a matrix, where $\mathcal{I}$ and $\mathcal{J}$ denote row indices and column indices, respectively. Then, $\boldsymbol{Z}[\mathcal{I};\mathcal{J}]$ represents a part of matrix $\boldsymbol{Z}$ indexed by $\mathcal{I}$ and $\mathcal{J}$. And $(\cdot)^\top$ denotes the transpose of matrices. A time series is represented as $\{y_t, t = 1, 2, \dots\}$ indexed by time t, which is a realization of a stochastic process $\{Y_t, t = 1, 2, \dots\}$. We also write them as $\{y_t\}$ and $\{Y_t\}$ for short.

2. Preliminaries

We first describe the framework for very-short-term wind power forecasting, for both point and probabilistic forecasting cases. Subsequently, we detail the challenges induced by missing values at both the model estimation and operational forecasting stages.

2.1. Problem formulation

Assume we have p wind farms in a region that can share information to improve forecasting accuracy, as suggested by Cavalcante et al. (2017). When $p = 1$, it reduces to the common single wind farm case. At wind farm n, let $y_{n,t} \in [0, P_n]$ (where P_n is its capacity) denote the wind power generation value at time t, which is a realization of the random variable $Y_{n,t}$. Let $\Omega_{n,t}$ denote the information tuple of wind farm n up to time t, which would contain values over previous time steps and possibly other relevant information such as weather observations and numerical weather forecasts. And let Ω_t represent the tuple that contains the information of all sites up to time t, i.e., $\Omega_t = (\Omega_{1,t}, \dots, \Omega_{p,t})$. Generally, the aim is to issue forecasts with lead time h, i.e., the characteristics of $Y_{1,t+1}, \dots, Y_{1,t+h}, \dots, Y_{p,t+1}, \dots, Y_{p,t+h}$, given information Ω_t. The forecasting task can be decoupled into several sub-problems, each of which focuses on a specific site and time, for instance forecasting the characteristics of $Y_{n,t+h}$ based on the whole information pool Ω_t. Then the point forecast for $Y_{n,t+h}$ given by a model $\mathcal{M}$ with parameters $\hat{\Theta}_t$ is usually defined as

$$\hat{y}_{n,t+h|t} = \mathbb{E}[Y_{n,t+h}|\mathcal{M}, \hat{\Theta}_t, \Omega_t], \tag{1}$$

where $\mathbb{E}[\cdot]$ denotes the expectation of random variables, and $\hat{\Theta}_t$ changes with time t. In this paper, let us assume that the stochastic process $\{Y_{1,t}, Y_{2,t}, \dots, Y_{p,t}\}$ is stationary. Then the density function $f_{Y_{1,t},\dots,Y_{p,t+h}}$ is invariant for changes in time (De Gooijer et al., 2017), which means that the parameters $\hat{\Theta}_t$ do not vary with time and are denoted as $\hat{\Theta}$. Then one can estimate the parameters based on collected data via statistical learning methods. We rewrite (1) as

$$\hat{y}_{n,t+h|t} = \mathbb{E}[Y_{n,t+h}|\mathcal{M}, \hat{\Theta}, \Omega_t]. \tag{2}$$

The probabilistic forecast for time $t + h$ given by $\mathcal{M}$ is communicated as a density function, i.e.,

$$\hat{f}_{n,t+h|t}(y) = f_{Y_{n,t+h}}(y|\mathcal{M}, \hat{\Theta}, \Omega_t). \tag{3}$$

Indeed, with the estimated density function at hand, one can easily obtain point forecast, via

$$\hat{y}_{n,t+h|t} = \int_y y \hat{f}_{n,t+h|t}(y)\, dy. \tag{4}$$

For simplicity of notation, let us focus on the predictive density $\hat{f}_{n,t+h|t}$ given the information set Ω_t at time t. We denote the input features as $\boldsymbol{x}_t$ and the realization of target $Y_{n,t+h}$ as y_t. The information one has access to, N sample pairs $(\boldsymbol{x}_1, y_1), \dots, (\boldsymbol{x}_N, y_N)$, serves as a basis for training. They can be written in the form of a matrix, i.e., $\boldsymbol{X} = [\boldsymbol{x}_1, \dots, \boldsymbol{x}_N]^\top$ as well as $\boldsymbol{Y} = [y_1, \dots, y_N]^\top$. The matrix $\boldsymbol{X}$ has dimensions $N \times pk$, whereas $\boldsymbol{Y}$ is a vector with N elements. Now the density forecast described in (3) boils down to conditional probability density function estimation, which is performed via statistical learning. In very-short-term WPF, one commonly uses past wind power generation values of length k as input features, i.e., a vector $[y_{n,t-k+1}, \dots, y_{n,t}]^\top \in [0, P_n]^k$ for the nth site. Therefore, considering all sites together, the vector of input features is given by

$$\begin{aligned}\boldsymbol{x}_t &= [y_{1,t-k+1}, \dots, y_{1,t}, \dots, y_{p,t-k+1}, \dots, y_{p,t}]^\top \\ &\in [0, P_1]^k \times [0, P_2]^k \times \dots \times [0, P_p]^k.\end{aligned}$$

Obviously, the features in $\boldsymbol{x}_t$ have some form of dependency, which breaks down the classical i.i.d. assumption in statistical learning. However, it is still common to place oneself in a regression framework for estimation and overlook this dependency issue, as has been done recently for global/local model estimation (Montero-Manso & Hyndman, 2021) and estimation in deep learning models (Benidis et al., 2022). The consequences are actually fairly mild in practice, since the fact that input features are not independent mainly affects the interpretability of regression coefficients and the ability to perform hypothesis testing (to assess whether coefficients are significantly different from 0). The fact that observation samples used as a basis for estimation are not i.i.d. mainly yields higher variance in coefficient estimates—an issue when dealing with small datasets, which is rarely the case today for most statistical and machine learning applications, including wind energy forecasting.

Based on a stationarity assumption, the sample pairs $(\boldsymbol{x}_1, y_1), \dots, (\boldsymbol{x}_N, y_N)$ can be regarded as identically distributed. For simplicity, we introduce two random variables, X and Y, for these samples. This allows us to model the joint distribution $f_{X,Y}(\boldsymbol{x}, y)$ via $\mathcal{M}$ with estimated parameters $\hat{\Theta}$, i.e., $f_{X,Y}(\boldsymbol{x}, y; \mathcal{M}, \hat{\Theta})$, and derive $f_{Y|X}(y|\boldsymbol{x})$ via the conditional probability formula:

$$\begin{aligned}f_{Y|X}(y|\boldsymbol{x}; \mathcal{M}, \hat{\Theta}) &= \frac{f_{X,Y}(\boldsymbol{x}, y; \mathcal{M}, \hat{\Theta})}{f_X(\boldsymbol{x}; \mathcal{M}, \hat{\Theta})} \\ &= \frac{f_{X,Y}(\boldsymbol{x}, y; \mathcal{M}, \hat{\Theta})}{\int_y f_{X,Y}(\boldsymbol{x}, y; \mathcal{M}, \hat{\Theta}) dy}.\end{aligned} \tag{5}$$

With the estimated joint distribution $f_{X,Y}(\boldsymbol{x}, y; \mathcal{M}, \hat{\Theta})$ at hand, at any time t, given contextual information $\boldsymbol{x}_t$, one can issue the forecast $\hat{f}_{Y|X}(y_t|\boldsymbol{x}_t; \mathcal{M}, \hat{\Theta})$ via (5). In this paper, $\mathcal{M}$ is set as an imputation model and implicitly defined by a collection of conditional distributions. Each conditional distribution is implemented by predictive mean matching that relies on a function, for instance g_j parameterized by $\hat{\theta}_j$. As we are considering the joint distribution now, we can concatenate $\boldsymbol{x}_t$ and y_t as $\boldsymbol{z}_t$, i.e., $\boldsymbol{z}_t =$

$[\boldsymbol{x}_t^\top, y_t]^\top$. Accordingly, the dataset is concatenated as the matrix $\boldsymbol{Z}$ of shape $N \times (pk+1)$, i.e.,

$$\boldsymbol{Z} = \begin{bmatrix} \boldsymbol{x}_1^\top & y_1 \\ \boldsymbol{x}_2^\top & y_2 \\ \vdots & \vdots \\ \boldsymbol{x}_N^\top & y_N \end{bmatrix} = \begin{bmatrix} \boldsymbol{z}_1^\top \\ \boldsymbol{z}_2^\top \\ \vdots \\ \boldsymbol{z}_N^\top \end{bmatrix}.$$

We refer to the ith row, jth column, and (i,j)-th entry of $\boldsymbol{Z}$ as $\boldsymbol{z}_i$, $\boldsymbol{Z}_j$, and $z_{i,j}$, respectively. And we introduce a random variable $Z = (X, Y)$ that concatenates X and Y, which contains $pk+1$ variables (recall that X has pk variables, as it represents information from p sites), i.e., $Z = (Z_1, Z_2, \dots, Z_{pk+1})$. Then the distribution of Z is modeled by $f_Z(\boldsymbol{z}; \mathcal{M}, \hat{\Theta})$. In particular, let Z_{-j} denote the collection of random variables in Z, except Z_j, i.e., $Z_{-j} = (Z_1, \dots, Z_{j-1}, Z_{j+1}, \dots, Z_{pk+1})$. Accordingly, let $\boldsymbol{z}_{-j}$ denote the realization of Z_{-j}.

We assume values are missing at random. This is to be understood in a way that is more general than data missing sporadically and at random times. More formally, missingness at random means that the fact that a data entry is missing or not is independent of the process itself, or of some exogenous process. For wind power applications, missing data might not be random when there are systematic sensor failures for power generation values below a given threshold, or systematic communication failures when wind comes from a given direction. In addition, missingness at random is not restricted to the case where data are missing at single times. It can also be for the case of data missing over time intervals (i.e., block missingness). This assumption of missingness at random is expected to be sound for wind power applications, though this should be confirmed on a case-by-case basis based on advanced data analysis.

Missing values are likely to occur in every element of $\boldsymbol{z}_t$. Let us introduce a vector $\boldsymbol{m}_t$ to indicate the missingness of $\boldsymbol{z}_t$. Concretely, $m_{t,j} = 1$ indicates that $z_{t,j}$ is missing, whereas $m_{t,j} = 0$ indicates that $z_{t,j}$ is observed. Accordingly, the matrix $\boldsymbol{M}$ indicates the missingness of $\boldsymbol{Z}$. Let $\mathcal{J}_{\boldsymbol{z}_t,M}$ denote the indices of missingness of $\boldsymbol{z}_t$, i.e., $\mathcal{J}_{\boldsymbol{z}_t,M} = \{j \mid m_{t,j} = 1\}$, and let $\mathcal{J}_{\boldsymbol{z}_t,O}$ denote the indices of observations, i.e., $\mathcal{J}_{\boldsymbol{z}_t,O} = \{j \mid m_{t,j} = 0\}$. Therefore, the observed and missing parts of $\boldsymbol{z}_t$ are represented by $\boldsymbol{z}_t[\mathcal{J}_{\boldsymbol{z}_t,O}]$ and $\boldsymbol{z}_t[\mathcal{J}_{\boldsymbol{z}_t,M}]$, which are written as $\boldsymbol{z}_t^{obs}$ and $\boldsymbol{z}_t^{mis}$ for simplicity. The corresponding random variables for $\boldsymbol{z}_t^{obs}$ and $\boldsymbol{z}_t^{mis}$ are denoted as Z^{obs} and Z^{mis}, respectively. When y_t is missing, $\boldsymbol{z}_t^{mis} = [\boldsymbol{x}_t^{mis\top}, y_t]^\top$, where $\boldsymbol{x}_t^{mis}$ is the missing part of $\boldsymbol{x}_t$. The corresponding random variables for $\boldsymbol{x}_t^{mis}$ are denoted as X^{mis}. For example, Fig. 1 presents the matrix $\boldsymbol{Z} = [z_{i,j}]_{4\times 4}$, where blue blocks indicate observations and yellow blocks indicate missing values. As shown, the first row of $\boldsymbol{Z}$ is denoted as $\boldsymbol{z}_1$, the second entry of which, i.e., $z_{1,2}$, is missing. Then, the indices of missing values and observations of $\boldsymbol{z}_1$ are $\mathcal{J}_{\boldsymbol{z}_1,M} = \{2\}$ and $\mathcal{J}_{\boldsymbol{z}_1,O} = \{1,3,4\}$. Accordingly, we have $\boldsymbol{z}_1^{obs} = [z_{1,1}, z_{1,3}, z_{1,4}]^\top$, $\boldsymbol{z}_1^{mis} = [z_{1,2}]$. The corresponding random variables for $\boldsymbol{z}_1^{obs}$ and $\boldsymbol{z}_1^{mis}$ are denoted as $Z^{obs} = (Z_1, Z_3, Z_4)$ and $Z^{mis} = Z_2$, respectively. Also, let $\mathcal{I}_{\boldsymbol{Z}_j,M}$ denote the indices of missing values in $\boldsymbol{Z}_j$, i.e., $\mathcal{I}_{\boldsymbol{Z}_j,M} = \{i \mid m_{i,j} = 1\}$, and let $\mathcal{I}_{\boldsymbol{Z}_j,O}$ denote the indices of observations in $\boldsymbol{Z}_j$, i.e., $\mathcal{I}_{\boldsymbol{Z}_j,O} = \{i \mid m_{i,j} = 0\}$. Then the missing and observed parts of $\boldsymbol{Z}_j$ are $\boldsymbol{Z}[\mathcal{I}_{\boldsymbol{Z}_j,M}; j]$ and $\boldsymbol{Z}[\mathcal{I}_{\boldsymbol{Z}_j,O}; j]$, which are respectively written as $\boldsymbol{Z}_j^{mis}$ and $\boldsymbol{Z}_j^{obs}$ for simplicity. In Fig. 1, $\boldsymbol{Z}_1$ represents the first column of $\boldsymbol{Z}$, the second entry of which is missing. Accordingly, we have $\mathcal{I}_{\boldsymbol{Z}_1,M} = \{2\}$, $\mathcal{I}_{\boldsymbol{Z}_1,O} = \{1,3,4\}$, $\boldsymbol{Z}_1^{obs} = [z_{1,1}, z_{3,1}, z_{4,1}]^\top$, and $\boldsymbol{Z}_1^{mis} = [z_{2,1}]$.

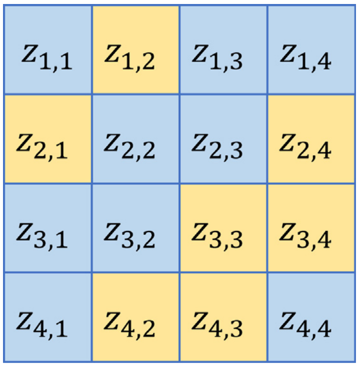

$z_{1,1}$	$z_{1,2}$	$z_{1,3}$	$z_{1,4}$
$z_{2,1}$	$z_{2,2}$	$z_{2,3}$	$z_{2,4}$
$z_{3,1}$	$z_{3,2}$	$z_{3,3}$	$z_{3,4}$
$z_{4,1}$	$z_{4,2}$	$z_{4,3}$	$z_{4,4}$

Fig. 1. Illustration of a dataset $\boldsymbol{Z}$. Here we take $p = 1$, $k = 3$, and $h = 1$ as an example. Blue blocks indicate observations, whereas yellow blocks indicate missing values. (For interpretation of the references to colour in this figure legend, the reader is referred to the web version of this article.)

Therefore, at the model estimation phase, we concatenate features and targets to form a training dataset $\boldsymbol{Z}^{tr}$ with some missing values, based on which an imputation model $\mathcal{M}$ is trained. At the operational forecasting phase, the input vector $\boldsymbol{x}_t$ at time t is available, part of which may be missing, and we focus on target y_t. Together they form $\boldsymbol{z}_t = [\boldsymbol{x}_t^\top, y_t]^\top$. Then $\boldsymbol{z}_t$ is imputed via the estimated model. For illustration, we present the training and test datasets for the single wind farm case in Fig. 2. In the training dataset, missingness occurs in both input features and targets. In the test dataset, all targets are systematically missing.

2.2. Challenge at the model estimation stage

Usually, the learning process of parameters in density estimation problems is based on maximum likelihood, which involves the computation of likelihood. However, in the presence of missing values, the likelihood is blended with missingness indicators. With the assumption that values are missing at random, the parameters of underlying distributions can be estimated based on observations only. Let Θ denote the true parameters of $\mathcal{M}$. Consider the likelihood of a sample $\boldsymbol{z}_t$. It is described as

$$f_Z(\boldsymbol{z}_t, \boldsymbol{m}_t; \mathcal{M}, \Theta) = f_Z(\boldsymbol{z}_t^{obs}, \boldsymbol{z}_t^{mis}, \boldsymbol{m}_t; \mathcal{M}, \Theta), \tag{6}$$

where $\boldsymbol{z}_t^{mis}$ is missing. The likelihood function can be marginalized with respect to $\boldsymbol{z}_t^{mis}$, i.e.,

$$\begin{aligned} f_{Z^{obs}}(\boldsymbol{z}_t^{obs}; \mathcal{M}, \Theta) &= \int f_{Z^{obs}, Z^{mis}}(\boldsymbol{z}_t^{obs}, \boldsymbol{z}_t^{mis}, \boldsymbol{m}_t; \mathcal{M}, \Theta) d\boldsymbol{z}_t^{mis} \\ &= \int f_{Z^{obs}, Z^{mis}}(\boldsymbol{z}_t^{obs}, \boldsymbol{z}_t^{mis}; \mathcal{M}, \Theta) d\boldsymbol{z}_t^{mis}. \end{aligned} \tag{7}$$

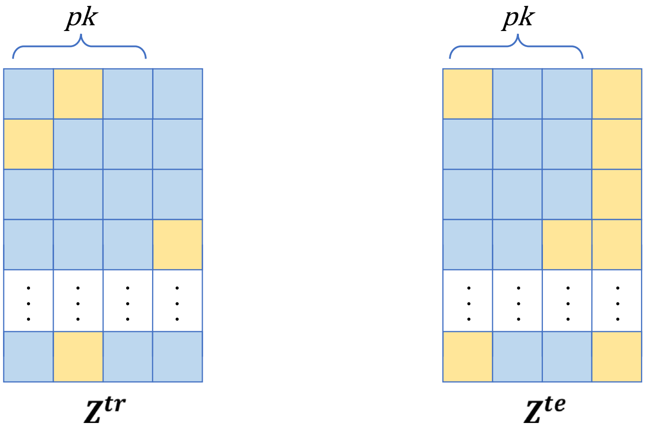

Fig. 2. Illustration of training and test datasets. Here we take $p = 1$, $k = 3$, and $h = 1$ as an example. Blue blocks indicate observations, whereas yellow blocks indicate missing values. (For interpretation of the references to colour in this figure legend, the reader is referred to the web version of this article.)

Therefore, to learn the parameters Θ, we must maximize the likelihood of observations only, i.e., $f_{Z^{obs}}(\boldsymbol{z}_i^{obs};\mathcal{M},\Theta)$. The estimate of Θ is denoted as $\hat{\Theta}$.

2.3. Challenge at the operational forecasting stage

In this section, we assume that we already have distribution $f_Z(\boldsymbol{z};\mathcal{M},\hat{\Theta})$ with estimated parameters $\hat{\Theta}$ at hand, and show how to issue forecasts at the operational forecasting stage. If $\boldsymbol{x}_t$ is fully observed, then $\boldsymbol{x}_t$ is the observed part of $\boldsymbol{z}_t$, i.e., $\boldsymbol{z}_t^{obs} = \boldsymbol{x}_t$, whereas the missing part of $\boldsymbol{z}_t$ is y_t. The forecast for y_t can be expressed as

$$f_{Y|X}(y_t|\boldsymbol{x}_t;\mathcal{M},\hat{\Theta}) = f_{Z^{mis}|Z^{obs}}(\boldsymbol{z}_t^{mis}|\boldsymbol{z}_t^{obs};\mathcal{M},\hat{\Theta}) = \frac{f_Z(\boldsymbol{z}_t^{obs},\boldsymbol{z}_t^{mis};\mathcal{M},\hat{\Theta})}{\int_{\boldsymbol{z}_t^{mis}} f_Z(\boldsymbol{z}_t^{obs},\boldsymbol{z}_t^{mis};\mathcal{M},\hat{\Theta})d\boldsymbol{z}_t^{mis}}. \tag{8}$$

In the presence of missing values, the forecasting task is to issue $f_{Y|Z^{obs}}(y|\boldsymbol{z}_t^{obs})$ by utilizing the distribution $f_Z(\boldsymbol{z};\mathcal{M},\hat{\Theta})$. Indeed, $\boldsymbol{z}_t^{mis}$ can be decomposed into $\boldsymbol{x}_t^{mis}$ and y_t, i.e.,

$$f_{Z^{mis}|Z^{obs}}(\boldsymbol{z}_t^{mis}|\boldsymbol{z}_t^{obs};\mathcal{M},\hat{\Theta}) = f_{Y,X^{mis}|Z^{obs}}(y_t,\boldsymbol{x}_t^{mis}|\boldsymbol{z}_t^{obs};\mathcal{M},\hat{\Theta}). \tag{9}$$

Then the desired $f_{Y|Z^{obs}}(y_t|\boldsymbol{z}_t^{obs};\mathcal{M},\hat{\Theta})$ is derived by marginalizing $f_{Z^{mis}|Z^{obs}}(\boldsymbol{z}_t^{mis}|\boldsymbol{z}_t^{obs};\mathcal{M},\hat{\Theta})$ with respect to $\boldsymbol{x}_t^{mis}$, i.e.,

$$f_{Y|Z^{obs}}(y_t|\boldsymbol{z}_t^{obs};\mathcal{M},\hat{\Theta}) = \int f_{Y,X^{mis}|Z^{obs}}(y_t,\boldsymbol{x}_t^{mis}|\boldsymbol{z}_t^{obs};\mathcal{M},\hat{\Theta})d\boldsymbol{x}_t^{mis}. \tag{10}$$

3. Forecasting with missing values via FCS

In this section, we develop a forecasting approach based on the proposed universal imputation strategy. For that, we employ the fully conditional specification approach, which in practice will be based on Gibbs sampling. It is described in the first part of the Section. This FCS approach requires a method to derive conditional distributions, which we describe in the second part. Eventually, it also relies on the choice for a regression model (random forests, here), covered in the third part of the section. Finally, we describe how the overall approach can be readily used for genuine forecasting with missing data.

3.1. Fully conditional specification method

Instead of defining a multivariate distribution $f_Z(\boldsymbol{z};\mathcal{M},\hat{\Theta})$ by assuming a specific distribution family, the FCS specifies a separate conditional distribution for each Z_j, just like a Gibbs sampler. Concretely, the conditional distribution for Z_j is modeled by g_j with parameters $\hat{\theta}_j$, and is denoted as $f_{Z_j|Z_{-j}}(z_j|\boldsymbol{z}_{-j};g_j,\hat{\theta}_j)$. Therefore, the model $\mathcal{M}$ is implemented via a bunch of models $\{g_j\}$, whereas $\hat{\Theta}$ is composed of all parameters $\{\hat{\theta}_j\}$. These parameters are estimated at the model estimation phase based on the training dataset $\boldsymbol{Z}^{tr}$. For simplicity of notation, we still use $\boldsymbol{Z}$ in what follows to show how to estimate the parameters. Intuitively, before estimating $\hat{\theta}_j$, one needs to impute the missing values of $\boldsymbol{Z}_{-j}$. Then parameters are estimated based on the imputed $\boldsymbol{Z}_{-j}$ and $\boldsymbol{Z}_j^{obs}$. With the estimated conditional distribution $f_{Z_j|Z_{-j}}(z_j|\boldsymbol{z}_{-j};g_j,\hat{\theta}_j)$, one can impute $\boldsymbol{Z}_j^{mis}$ based on the corresponding conditionals in $\boldsymbol{Z}_{-j}$. That is, both the estimation of $\hat{\theta}_j$ and the imputation of $\boldsymbol{Z}_j^{mis}$ are based on the imputed $\boldsymbol{Z}_{-j}$. Obviously, the imputation of any column of $\boldsymbol{Z}_{-j}$, for instance $\boldsymbol{Z}_q$, relies on its conditional distribution $f_{Z_q|Z_{-q}}(z_q|\boldsymbol{z}_{-q};g_q,\hat{\theta}_q)$, which requires $\boldsymbol{Z}_j^{mis}$ to be imputed. In other words, the estimation of $\hat{\theta}_j$ and the imputation of $\boldsymbol{Z}_{-j}$ are coupled with each other. If one performs the parameter estimation and imputation sequentially for $j = 1, 2, \ldots, pk+1$, the estimation of $\hat{\theta}_j$ can only use the initial imputation of $\boldsymbol{Z}_{j+1}^{mis}, \ldots, \boldsymbol{Z}_{pk+1}^{mis}$. The updated imputation of $\boldsymbol{Z}_{j+1}^{mis}, \ldots, \boldsymbol{Z}_{pk+1}^{mis}$, given by their estimated conditional distributions, cannot be used for the estimation of $\hat{\theta}_j$. Therefore, we perform the imputation of $\boldsymbol{Z}_j$ and the estimation of $\hat{\theta}_j$ in an iterative manner. Then at the next iteration, the updated imputation of $\boldsymbol{Z}_{j+1}^{mis}, \ldots, \boldsymbol{Z}_{pk+1}^{mis}$ can be used for the estimation of $\hat{\theta}_j$. For

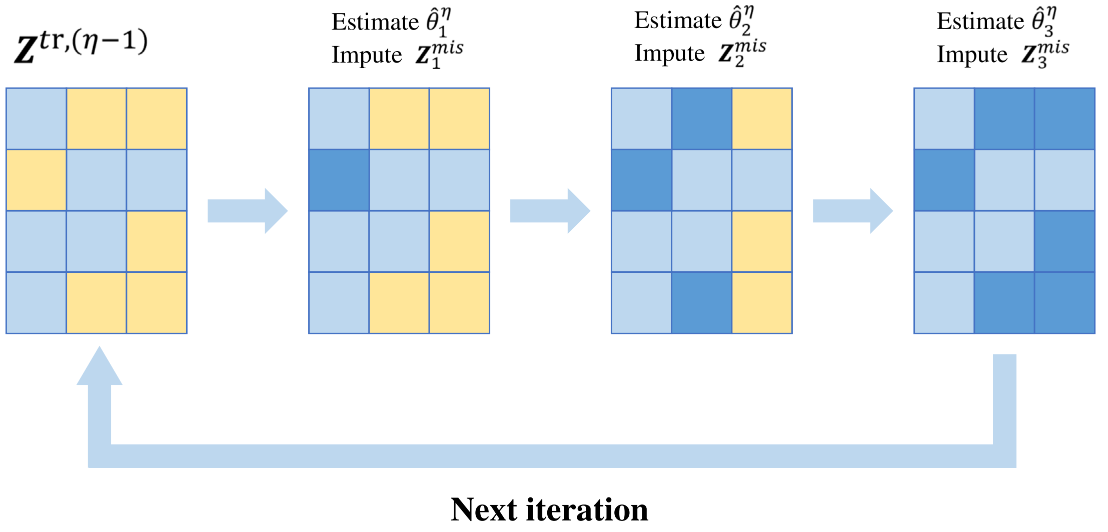
$\mathbf{Z}^{tr,(\eta-1)}$
Estimate $\hat{\theta}_1^{\eta}$
Impute $\mathbf{Z}_1^{mis}$
Estimate $\hat{\theta}_2^{\eta}$
Impute $\mathbf{Z}_2^{mis}$
Estimate $\hat{\theta}_3^{\eta}$
Impute $\mathbf{Z}_3^{mis}$
Next iteration

Fig. 3. Illustration of the η-th iteration at the training stage. Light blue blocks indicate observations, yellow blocks indicate missing values, and dark blue blocks indicate imputation. (For interpretation of the references to colour in this figure legend, the reader is referred to the web version of this article.)

example, we denote the estimated parameters $\hat{\theta}_j$ at the η-th iteration as $\hat{\theta}_j^{(\eta)}$, and the imputed complete column as $\mathbf{Z}_j^{(\eta)}$. At the $\eta+1$-th iteration, $\mathbf{Z}_{j+1}^{(\eta)}, \ldots, \mathbf{Z}_{pk+1}^{(\eta)}$ can be used for the estimation of $\hat{\theta}_j^{(\eta+1)}$. Before the iterative estimation, all missing values are initially imputed as 0; therefore, each column $\mathbf{Z}_j$ becomes complete and is written as $\mathbf{Z}_j^{(0)}$. After all iterations, the ultimate estimation for θ_j is denoted as $\hat{\theta}_j$. Here we set the stopping criterion as the round of iteration, as suggested by Van Buuren et al. (2006). The caveat is that the FCS method cannot guarantee the existence of a joint distribution. Luckily this is a relatively minor problem in practice, especially when the missing rate is modest. We illustrate the steps of the η-th iteration in Fig. 3.

Concretely, at the η-th iteration, before estimating $\hat{\theta}_j^{(\eta)}$, we have $\mathbf{Z}_1^{(\eta)}, \cdots, \mathbf{Z}_{j-1}^{(\eta)}, \mathbf{Z}_{j+1}^{(\eta-1)}, \cdots, \mathbf{Z}_{pk+1}^{(\eta-1)}$ at hand, which are written compactly as $\mathbf{Z}_{-j}^{(\eta)}$ in the form of a matrix, i.e.,

$$\mathbf{Z}_{-j}^{(\eta)} = [\mathbf{Z}_1^{(\eta)}, \ldots, \mathbf{Z}_{j-1}^{(\eta)}, \mathbf{Z}_{j+1}^{(\eta-1)}, \ldots, \mathbf{Z}_{pk+1}^{(\eta-1)}]. \tag{11}$$

Then $\hat{\theta}_j^{(\eta)}$ is estimated based on $\mathbf{Z}_{-j}^{(\eta)}$ and $\mathbf{Z}_j^{obs}$ via maximum likelihood:

$$\hat{\theta}_j^{(\eta)} = \arg\max_{\theta_j} \sum_{i \in \mathcal{I}_{j,obs}} \log f_{Z_j|Z_{-j}}(z_{i,j}|\mathbf{z}_{i,-j}^{(\eta)}; g_j, \theta_j). \tag{12}$$

Thus we derive the estimated conditional distribution $f_{Z_j|Z_{-j}}(z_j|\mathbf{z}_{-j}; g_j, \hat{\theta}_j^{(\eta)})$, based on which we can impute $\mathbf{Z}_j^{mis}$. For instance, to impute the value $z_{i,j}$ in $\mathbf{Z}_j^{mis}$, we sample from $f_{Z_j|Z_{-j}}(z_j|\mathbf{z}_{i,-j}; g_j, \hat{\theta}_j^{(\eta)})$, which is described as

$$z_{i,j}^{(\eta)} \sim f_{Z_j|Z_{-j}}(z_j|\mathbf{z}_{-j}; g_j, \hat{\theta}_j^{(\eta)}), \quad i \in \mathcal{I}_{j,mis}. \tag{13}$$

As $\mathbf{Z}_j^{obs}$ is observed, we do not change the values, i.e.,

$$z_{i,j}^{(\eta)} = z_{i,j}^{(\eta-1)}, \quad i \in \mathcal{I}_{j,obs}. \tag{14}$$

Then we write all $z_{i,j}^{(\eta)}$ in the form of a vector, which is denoted as $\mathbf{Z}_j^{(\eta)}$, i.e.,

$$\mathbf{Z}_j^{(\eta)} = [z_{1,j}^{(\eta)}, \ldots, z_{N,j}^{(\eta)}]^\top. \tag{15}$$

This procedure proceeds sequentially for $j = 1, \ldots, pk+1$. We note that the method can be executed multiple times in parallel to obtain multiple imputations. Further, the model g_j for $f_{Z_j|Z_{-j}}(z_j|\mathbf{z}_{-j}; g_j, \hat{\theta}_j)$ needs to be specified, as described in the next section.

3.2. Predictive mean matching

In this paper, $f_{Z_j|Z_{-j}}(z_j|\mathbf{z}_{-j}; \hat{\theta}_j, g_j)$ is specified based on predictive mean matching (Little & Rubin, 2019), which is free of distributional assumptions. Specifically, here g_j is not a real distribution model, but specified as a regression model. The distribution is given by a sampling procedure based on g_j. For each missing entry, we form a set of candidates from complete cases whose predicted values are close to the predicted value for the missing entry. Now we use parameters θ_j to specify the regression model g_j that maps $\mathbf{z}_{-j}$ to z_j, i.e.,

$$z_j = g_j(\mathbf{z}_{-j}; \theta_j) + \epsilon_j, \tag{16}$$

where ϵ_j represents noise. We illustrate the key operations of this method in Fig. 4, i.e., the training of the regression model and the prediction of candidates. That is, we estimate parameters $\hat{\theta}_j$ based on training datasets $\mathbf{Z}_{-j}^{tr}$ and $\mathbf{Z}_j^{tr}$. With the estimated model, we predict targets for $\mathbf{Z}_{-j}^{tr}$ and $\mathbf{Z}_{-j}^{te}$, which are called candidates, written as $\hat{\mathbf{Z}}_j^{tr}$ and $\hat{\mathbf{Z}}_j^{te}$, respectively. Then for each entry of $\hat{\mathbf{Z}}_j^{te}$, we form a set of its d closest candidates in $\hat{\mathbf{Z}}_j^{tr}$, from which we perform random sampling to obtain imputations.

At the η-th iteration of FCS, the regression model is trained based on $\mathbf{Z}_{-j}^{(\eta)}[\mathcal{I}_{j,obs}, :]$ and $\mathbf{Z}_j^{obs}$ by minimizing the

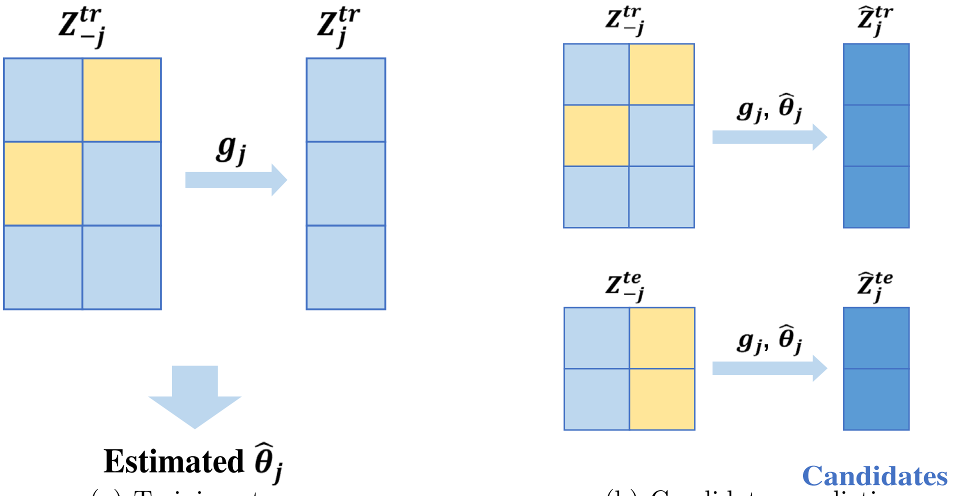

(a) Training stage (b) Candidates prediction

Fig. 4. Illustration of key components of predictive mean matching.

loss, i.e.,

$$\hat{\theta}_j^{(\eta)} = \arg\min_{\theta_j} \sum_{i \in \mathcal{I}_{j,obs}} \ell(z_{i,j} - g_j(\boldsymbol{z}_{i,-j}^{(\eta)}; \theta_j)), \tag{17}$$

where $\ell(\cdot)$ is the mean squared error function. Then we predict a candidate value for each $\boldsymbol{z}_{i,-j}^{(\eta)}$ via the trained regression model, which is denoted as $\hat{z}_{i,j}^{(\eta)}$, i.e.,

$$\hat{z}_{i,j}^{(\eta)} = g_j(\boldsymbol{z}_{i,-j}^{(\eta)}; \hat{\theta}_j^{(\eta)}). \tag{18}$$

Together, they are written in the form of a vector as $\hat{\boldsymbol{Z}}_j^{(\eta)}$, which is expressed as

$$\hat{\boldsymbol{Z}}_j^{(\eta)} = [\hat{z}_{1,j}^{(\eta)}, \hat{z}_{2,j}^{(\eta)}, \ldots, \hat{z}_{N,j}^{(\eta)}]^\top. \tag{19}$$

To impute $\boldsymbol{Z}_j^{mis}$, let us focus on each of its missing entries, for instance $z_{i_m,j}$, $i_m \in \mathcal{I}_{j,mis}$, whose candidate is $\hat{z}_{i_m,j}^{(\eta)}$. Then we find the d nearest candidates from $\hat{\boldsymbol{Z}}_j^{(\eta)}[\mathcal{I}_{j,obs}]$ for which $|\hat{z}_{i_m,j}^{(\eta)} - \hat{z}_{i,j}^{(\eta)}|$, $i_m \in \mathcal{I}_{j,mis}$, $i \in \mathcal{I}_{j,obs}$ is minimal. Suppose the d candidates are

$$\hat{z}_{i_1,j}^{(\eta)}, \hat{z}_{i_2,j}^{(\eta)}, \ldots, \hat{z}_{i_d,j}^{(\eta)}, \quad i_1, i_2, \ldots, i_d \in \mathcal{I}_{j,obs},$$

which can be written in the form of a set as $\mathcal{C}_{i,j}$, i.e., $\mathcal{C}_{i,j} = \{\hat{z}_{i_1,j}^{(\eta)}, \hat{z}_{i_2,j}^{(\eta)}, \ldots, \hat{z}_{i_d,j}^{(\eta)}\}$. Finally, we obtain imputation for $z_{i,j}$, $i \in \mathcal{I}_{j,mis}$ by sampling from $\mathcal{C}_{i_m,j}$ and denote it as $z_{i_m,j}^{(\eta)}$, i.e.,

$$z_{i_m,j}^{(\eta)} \sim \mathcal{C}_{i,j}, \quad i_m \in \mathcal{I}_{j,mis}. \tag{20}$$

Indeed, the set $\mathcal{C}_{i_m,j}$ provides an empirical distribution for $z_{i_m,j}$, $i_m \in \mathcal{I}_{j,mis}$. The operations described from (17) to (20) correspond the conceptual description in (12) and (13). After all iterations, the final candidates corresponding to the training dataset are denoted as $\hat{\boldsymbol{Z}}_j$, which are prepared for the use of sampling at the operational forecasting stage. In particular, missing values can be directly imputed via (18) when only point forecasts are needed.

3.3. *Random forests*

Indeed, the model described in (16) can be specified as any regression model, such as linear regression, random forests, etc. In this paper, it is specified as a random forest, as tree models usually perform well in practice (Januschowski, Wang, Torkkola, Erkkilä, & Gasthaus, 2021). It grows B regression trees, each of which is trained on bootstrap samples from training data. Hence, the regression model that maps variables $\boldsymbol{z}_{-j}$ to z_j is described as

$$g_j(\boldsymbol{z}_{-j}; \hat{\theta}_j) = \frac{1}{B} \sum_{b=1}^{B} g_{j,b}(\boldsymbol{z}_{-j}), \tag{21}$$

where $g_{j,b}(\boldsymbol{z}_{-j})$ is a regression tree. The splitting variable and splitting points of regression trees are often determined by the CART algorithm. Details about the CART algorithm can be found in Hastie, Tibshirani, and Friedman (2001). Suppose we have already partitioned the variables into M regions, i.e., $R_1, R_2, \ldots, R_M$. And we model the target as a constant c_m in each region. The regression function is described as

$$g_{j,b}(\boldsymbol{z}_{-j}) = \sum_{m=1}^{M} c_m I(\boldsymbol{z}_{-j} \in R_m), \tag{22}$$

where $I(\cdot)$ is the indicator function. In particular, c_m is estimated as the average of targets z_j in the region R_m, i.e.,

$$\hat{c}_m = \frac{1}{|\mathcal{I}_{R_m}|} \sum_{i \in \mathcal{I}_{R_m}} z_{i,j}, \tag{23}$$

where $\mathcal{I}_{R_m} = \{i \mid \boldsymbol{z}_{i,-j} \in R_m\}$. The model grows like a binary tree. To begin with, we consider that the space is split at variable Z_a, $a \in \{1, \ldots, j-1, j+1, \ldots, pk+1\}$ and point s. Then we obtain two halves:

$$R_1(a,s) = \{\boldsymbol{z}_{-j} | z_a \leq s\}, \; R_2(a,s) = \{\boldsymbol{z}_{-j} | z_a > s\}. \tag{24}$$

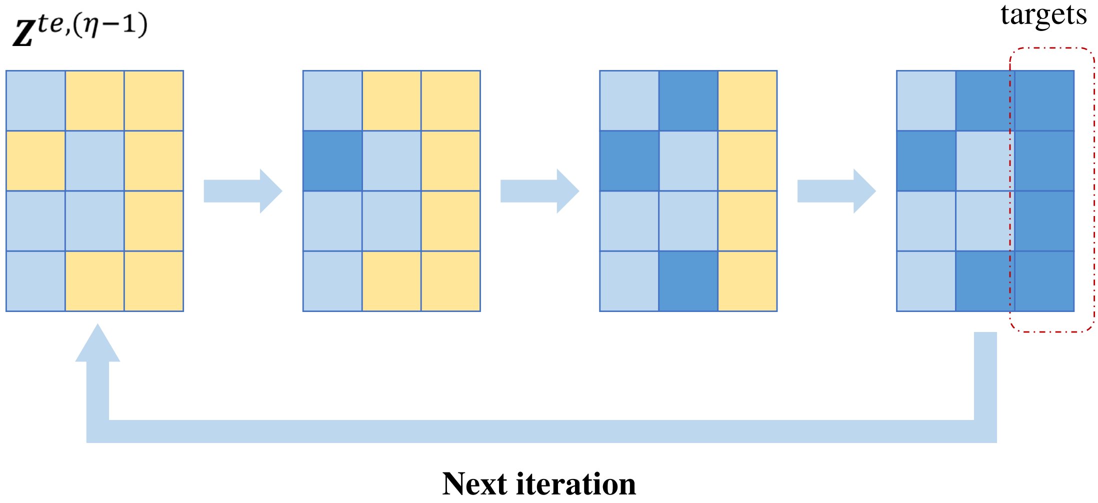

Fig. 5. Illustration of the η-th iteration at the operational forecasting stage. Light blue blocks indicate observations, yellow blocks indicate missing values, and dark blue blocks indicate imputation (forecasting). (For interpretation of the references to colour in this figure legend, the reader is referred to the web version of this article.)

It is fulfilled by a greedy algorithm, i.e.,

$$\min_{a,s}\left[\min_{c_1}\sum_{z_{i,-j}\in R_1(a,s)}\ell(z_{i,j}-c_1)+\min_{c_2}\sum_{z_{i,-j}\in R_2(a,s)}\ell(z_{i,j}-c_2)\right]. \tag{25}$$

We repeat the splitting process in the two generated regions, and stop only when the minimum node size is reached.

3.4. Forecasting stage

After training the imputation model, we obtain a collection of estimated random forests $\{g_j\}$ with parameters $\{\hat{\theta}_j\}$ and candidates $\{\hat{\boldsymbol{Z}}_j\}$. At the operational forecasting stage, we feed sample $\boldsymbol{z}_t = [\boldsymbol{x}_t^\top, y_t]^\top$ (y_t is missing by default) into the estimated imputation model, and iteratively impute each missing value in $\boldsymbol{z}_t$ according to (11) and (13)–(15), as illustrated in Fig. 5. Compared to the training stage, the parameters are now fixed; thus we only conduct iterative imputation here. Particularly, L equally likely imputations for $\boldsymbol{z}_t$ are obtained, which are written as

$\tilde{\boldsymbol{z}}_t^1, \tilde{\boldsymbol{z}}_t^2, \dots, \tilde{\boldsymbol{z}}_t^L$.

Indeed, here $\boldsymbol{z}_t^{obs} = \boldsymbol{x}_t^{obs}$, $\boldsymbol{z}_t^{mis} = [\boldsymbol{x}_t^{mis\top}, y_t]^\top$. That is, $\boldsymbol{z}_t^{mis}$ is imputed by realizations from the estimated distribution $f_{X^{mis},Y|X^{obs}}(\boldsymbol{z}_t^{mis}, y_t|\boldsymbol{x}_t^{obs}; \mathcal{M}, \hat{\Theta})$. To get an empirical distribution for $f_{Y|X^{obs}}(y_t|\boldsymbol{x}_t^{obs}; \mathcal{M}, \hat{\Theta})$, we just fetch the corresponding value for y_t in each $\tilde{\boldsymbol{z}}_t^i$, i.e., the last entry of $\tilde{\boldsymbol{z}}_t^i$, which is denoted as $\tilde{y}_t^i$, i.e.,

$$\tilde{y}_t^i = \tilde{z}_{t,pk+1}^i, \quad i = 1, \dots, L. \tag{26}$$

Recall that y_t is the realization of the random variable $Y_{n,t+h}$. That is, $\tilde{y}_t^i$ is the realization from $f_{Y_{n,t+h|t}}(y|\boldsymbol{x}_t; \mathcal{M}, \hat{\Theta})$. Thus we rewrite $\tilde{y}_t^i$ as $\tilde{y}_{n,t+h|t}^i$, all of which form a set, i.e.,

$\{\tilde{y}_{n,t+h|t}^1, \tilde{y}_{n,t+h|t}^2, \dots, \tilde{y}_{n,t+h|t}^L\}$.

Note that (26) is a surrogate of (10), which serves as marginalization operation when L is quite large. The point forecast $\hat{y}_{n,t+h|t}$ is given as an average, which is expressed as

$$\hat{y}_{n,t+h|t} = \frac{1}{L}\sum_{i=1}^{L}\tilde{y}_{n,t+h|t}^i. \tag{27}$$

4. Simulation study

Before validating the proposed approach on real data, we illustrate its applicability to point forecasting based on two related simulated processes, i.e., the autoregressive (AR) process and vector autoregressive (VAR) process. The results are assessed in terms of the root-mean-square error (RMSE) here. Let $\mathcal{I}_{y,obs}$ denote the indices of observations in the test set. Then the RMSE on the test set is derived as follows:

$$\text{RMSE} = \sqrt{\frac{1}{|\mathcal{I}_{y,obs}|}\sum_{t\in\mathcal{I}_{y,obs}}(y_t - \hat{y}_t)^2}, \tag{28}$$

where y_t denotes the observation at time t, $\hat{y}_t$ denotes the point forecast at time t, and $|\mathcal{I}_{y,obs}|$ is the number of observed samples in the test set. In each case, we remove parts of generated data at random to simulate missingness, where the missing rate is varied from 5% to 50%. Situations where missing rates are larger than 50% are regarded as impractical and thus not included in the study. Then, 80% of the data are used as the training set, and the other 20% are used as the test set for genuine forecasting validation. The missingness simulation and model validation are replicated 100 times for each missing rate.

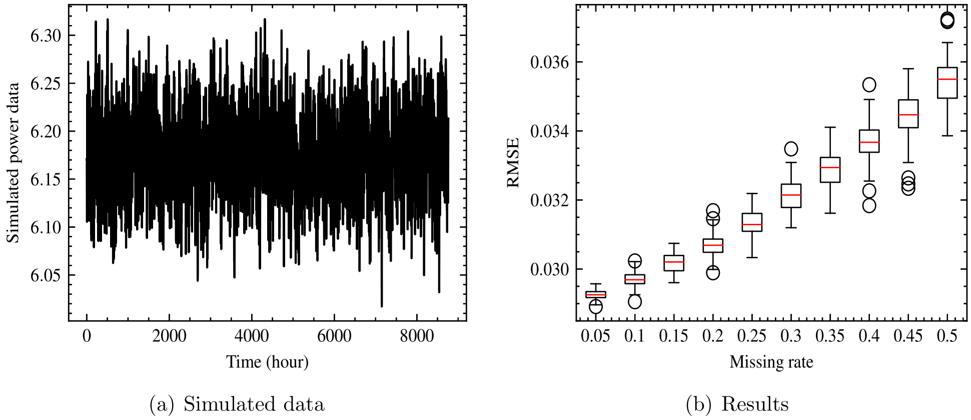

(a) Simulated data

(b) Results

Fig. 6. (a) Example of a simulated time series with an AR process (single replicate). (b) Box plot of one-step-ahead RMSE in the presence of missing values based on AR simulated data with respect to different missing rates (based on Monte Carlo simulations with 100 replicates).

4.1. AR process

In this case, we model an AR process of order 2, i.e.,

$$Y_t = \alpha_0 + \alpha_1 Y_{t-1} + \alpha_2 Y_{t-2} + \epsilon_t,$$

where α_0 is a constant, α_1 and α_2 are parameters, and ϵ_t is white noise centered on 0. Let us set $\boldsymbol{\alpha}^\top$ as $[1,\ 0.33,\ 0.5]^\top$, and ϵ_t to follow the Gaussian $\mathcal{N}(0, 0.01)$. Concretely, we simulate a time series of length 8760, corresponding to a year of data with one-hour resolution, as presented in Fig. 6(a). The input features $\boldsymbol{x}_t$ have two dimensions, and the target y_t has one dimension. Specifically, the imputation model is trained by 10 iterations, as suggested by Van Buuren et al. (2006). The RMSE values with respect to different missing rates are shown in Fig. 6(b). Intuitively, missing values lead to an increase in RMSE, and higher missing rates lead to a larger RMSE.

Since the experiments at each missing rate are replicated 100 times, we obtain the variance of RMSE at each missing rate. As the missing rate increases, the variance of RMSE also increases, because the influence on training varies to a larger extent when the missing rate is high.

4.2. VAR process

We model a VAR process of order 2, i.e.,

$$\begin{aligned} Y_{1,t} &= \alpha_0 + \alpha_{1,1} Y_{1,t-1} + \alpha_{1,2} Y_{1,t-2} + \alpha_{2,1} Y_{2,t-1} \\ &\quad + \alpha_{2,2} Y_{2,t-2} + \epsilon_{1,t}, \\ Y_{2,t} &= \beta_0 + \beta_{1,1} Y_{1,t-1} + \beta_{1,2} Y_{1,t-2} + \beta_{2,1} Y_{2,t-1} \\ &\quad + \beta_{2,2} Y_{2,t-2} + \epsilon_{2,t}, \end{aligned}$$

where $\boldsymbol{\alpha}_1^\top = [1,\ 0.88,\ -0.1,\ 0.15,\ -0.14]^\top$, $\boldsymbol{\alpha}_2^\top = [1,\ 0.69,\ -0.05,\ 0.07,\ -0.23]^\top$, $\epsilon_{1,t} \sim \mathcal{N}(0, 0.01)$, and $\epsilon_{2,t} \sim \mathcal{N}(0, 0.01)$. We still simulate time series of length 8760 and present them in Fig. 7(a). In this case, we focus on forecasting the future value of $Y_{1,t}$ by using previous realizations of both series. Now the input features $\boldsymbol{x}_t$ have elements, whereas the target y_t has only one dimension. We still train the imputation model with 10 iterations.

As a starting point, we assume that there are no missing values in series $\{y_{2,t}\}$ and only vary the missing rate for $\{y_{1,t}\}$. The overall RMSE values are presented in Fig. 7(b). As with the AR case, the RMSE and its variance increase as the missing rate increases. For comparison, we consider two other scenarios, i.e., only using features from $\{y_{1,t}\}$, and simulating missingness for both $\{y_{1,t}\}$ and $\{y_{2,t}\}$, the results of which are respectively shown in Fig. 7(c) and (d). Comparing Fig. 7(b) and (c), we observe that the RMSE in Fig. 7(b) is lower, which translates into saying that forecasting can be improved by using information from correlated series. However, as shown in Fig. 7(d), the benefit of using features from $\{y_{2,t}\}$ is still noticeable when the missing rate of $\{y_{2,t}\}$ is not too high. When the missing rate of $\{y_{2,t}\}$ is higher than 30%, using the features of $\{y_{2,t}\}$ will even hamper the performance.

5. Case study

Besides the above simulation study, we further validate our approach based on real-world data from the USA. The case study considers a typical forecasting setup, where some data are used for estimating model parameters (training set) and the remainder are used for genuine out-of-sample forecast verification (test set). Both point and probabilistic forecasting are considered. Also, since the dataset gathers data for multiple wind farms in a limited area, we can look at the case of employing univariate approaches (i.e., the use of local data only), but also at the case where data from surrounding wind farms are used to improve forecasts. In that case, it is intuitively expected that one is further exposed to the likelihood and potential consequences of missing data. Note that the goal of this case study is not to pick and choose the best model and forecasting approach, but instead to show the impact of missing values on forecasting and the effectiveness of the proposed approach to accommodate those. In the following, we first describe the dataset and our experimental setup, the forecast verification framework, and the benchmark approaches. The results obtained are then described and discussed. Codes and data[1] are publicly available.

[1] https://github.com/honglinwen/Forecasting-with-missing-values.git

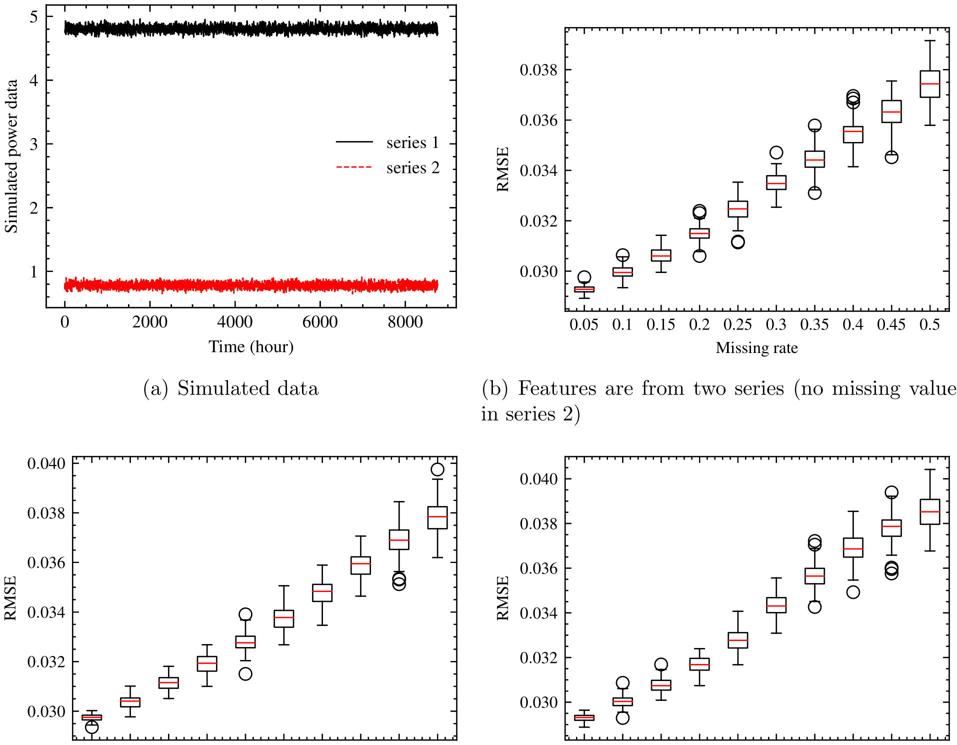

(a) Simulated data

(b) Features are from two series (no missing values in series 2)

(c) Features are only from series 1

(d) Features are from two series (with missing values in series 2)

Fig. 7. (a) Simulated time series of the VAR process. (b) Box plot of one-step-ahead RMSE based on VAR simulated data with respect to different missing rates for series 1 (Monte Carlo with 100 replications). (c) Box plot of one-step-ahead RMSE based on series 1 with respect to different missing rates for series 1 (Monte Carlo with 100 replications). (d) Box plot of one-step-ahead RMSE based on VAR simulated data with respect to different missing rates for both series (Monte Carlo with 100 replications).

5.1. Data description

Data from the USA are generated by the Wind Integration National Dataset (WIND) Toolkit (Draxl, Clifton, Hodge, & McCaa, 2015), which are therefore not completely real but capture the dynamics of wind power generation. Indeed, there are no missing values in this dataset. Thus, we randomly remove some values to simulate missingness, based on which all models are estimated and validated. Specifically, the dataset contains data on three wind farms located in South Carolina, within a 150 km area. The spatiotemporal dynamics among the wind farms suggest that one could use data from nearby wind farms to improve the forecasts. The dataset comprises data over seven years, from 2007 to 2013, with an hourly temporal resolution. All wind power measurements are normalized by their corresponding capacities.

5.2. Experimental setup

5.2.1. Different types of case studies

Based on the data described above, we concentrate on both point and probabilistic forecasting in three different types of case studies, representing alternative approaches to forecasting (local data only, and with data from surrounding wind farms), as well as different types of missingness, i.e., sporadic and block missingness. We also consider forecasting with lead times from $k = 1$ to 6 steps ahead. More precisely, these cases are described as follows:

Case 1: Forecasting at a single site, using local data only (hence, with an autoregressive model). Data are missing sporadically and randomly on a pointwise basis. The rates of missingness are 10% and 20%, respectively, to investigate the performance of the approach conditional on the amount of missing data.

Case 2: Forecasting at a single site using local data only (hence, with an autoregressive model). Data are missing over given time intervals (block missingness) though at random. The number of blocks with missing data is set to 600. These are randomly located over the dataset. The length of the block with missing data is random and uniformly distributed between 5 to 30 time steps.

Case 3: Forecasting at a chosen site, but using data from both that site and nearby sites (hence, with a vector autoregressive model). The two types of missingness mentioned above (pointwise and block missingness) are considered.

In all three cases, when issuing a forecast at time t for lead time $t+k$, lagged observations are used as input features (since we are using autoregressive models). As feature selection is not the focus of this paper, we performed a preliminary study to select lags based on training data. As a result, we work in the following with autoregressive models with six lagged observations (so, from $t-5$ to t). The generalized logit-normal transform proposed by Pinson (2012) is further employed as a preprocessing stage to accommodate the double-bounded nature of wind power generation time series (i.e., nonlinear and with the variance of residuals conditional upon the mean level).

5.2.2. Forecast verification: Relevant scores and diagnostic tools

The quality of point forecasts is commonly evaluated with an RMSE criterion (consistent with the use of a quadratic loss in learning and forecast verification), whereas the quality of probabilistic forecasts is most often assessed by using the continuous ranked probability score (CRPS). Given a lead time h, we denote the cumulative density function for wind power generation Y_{t+h}, predicted at time t for time $t+h$, as F_{t+h}. Then the CRPS for the predicted F_{t+h} and corresponding observation y_{t+h} is defined as

$$\mathrm{CRPS}(F_{t+h}, y_{t+h}) = \int_y \left(F_{t+h}(y) - \mathbb{1}(y - y_{t+h})\right)^2 dy, \tag{29}$$

where $\mathbb{1}(\cdot)$ is a unit step function at the location of the observation y_{t+h} (also known as a Heaviside function), which can be regarded as the empirical cumulative density function of the observation y_{t+h}. Eventually, given the lead time h, we report the average CRPS value over all forecast–verification pairs, i.e.,

$$\mathrm{CRPS}_h = \frac{1}{|\mathcal{I}_{y,obs}|} \sum_{t+h \in \mathcal{I}_{y,obs}} \mathrm{CRPS}(F_{t+h}, y_{t+h}). \tag{30}$$

Besides the use of a proper skill score like the CRPS, which is informative about the overall skill and quality of the probabilistic forecasts (in the form of predictive densities), we also assess the probabilistic calibration of the predictive densities with reliability diagrams. For an extensive description of such reliability diagrams and their use in the assessment of probabilistic calibration, the reader is referred to Pinson, McSharry, and Madsen (2010). In parallel, in order to see how the probabilistic forecasts concentrate information, their sharpness is evaluated by calculating the width of central prediction intervals. That is, for a given nominal coverage rate $1-\beta$, these central prediction intervals are bounded by quantiles with nominal levels $\beta/2$ and $1-\beta/2$. For a general overview of probabilistic forecast verification, see Gneiting, Balabdaoui, and Raftery (2007).

5.2.3. Benchmarks

In general, we use three categories of benchmarks: the climatology/persistence method, an ITP approach, and a UI approach with a distributional assumption. For point forecasting, the persistence method uses the latest observation as the forecast. To implement the ITP approach, we respectively use mean imputation and advanced regression-based imputation, namely MissForest (Stekhoven & Bühlmann, 2012), in the preprocessing procedure and employ a random forest as the backbone regression model, which are abbreviated as RF-M and RF-R, respectively. The state-of-the-art model DeepAR (Salinas et al., 2020) is adopted, which uses intermediate results of the long short-term memory model to impute missing values at both the model estimation and operational stages. The copula-based imputation model proposed by Zhao and Udell (2020) is adopted to implement the UI approach. It is also a multiple imputation model, though it relies on a distributional assumption. The retraining approach (Tawn et al., 2020) is used as a benchmark model, which consists in retraining the model without missing features. We also consider a reference model that is implemented by a random forest and trained based on the complete dataset, which is abbreviated as RF-C. The benchmark models for point forecasting, as well as the abbreviations used, are listed in Table 1.

As for probabilistic forecasting, climatology is set as a naive benchmark. It utilizes the empirical distribution of all historical values to communicate the probability distribution of future wind power generation. To implement the ITP approach, a model with the Gaussian distributional assumption and a QR model are adopted as backbone models. In particular, the base model chosen for QR is the gradient boosting machine, which supports QR and ranks highly on leaderboards of recent forecast competitions (Januschowski et al., 2021), including the GEFCom 2014 (Landry et al., 2016), for instance. For the model with the Gaussian distributional assumption, we use a neural network to estimate the shape parameters of Gaussian distributions. The QR model with regression-based imputation as preprocessing is abbreviated as QR-R, while the Gaussian models with mean and regression-based imputation are abbreviated as Gauss-M and Gauss-R, respectively. Again, the DeepAR model (Salinas et al., 2020) is used as a benchmark, since it is allowed to communicate Gaussian densities. The UI approach is still implemented via the copula-based model. We set the QR model trained based on the complete dataset as a reference, which is abbreviated as QR-C. The benchmark models for probabilistic forecasting, as well as the corresponding abbreviations, are also collated in Table 1.

5.3. Results and discussion

Results that correspond to the aforementioned three cases are respectively reported in the following three subsections, followed by further discussion.

5.3.1. Case 1

Emphasis is first placed on sporadic missingness, i.e., for the case where single values are missing at random times.

Table 1
Abbreviations for point and probabilistic forecasting benchmark models.

Abbreviation	Description (point forecasting)
RF-M	Random forest with the mean imputation as preprocessing
RF-R	Random forest with the regression-based imputation as preprocessing
Copula	Copula-based imputation model within universal imputation strategy
DeepAR	Deep learning model that uses intermediate results to impute missing values
RF-C	Random forest trained based on the complete dataset
Abbreviation	**Description (probabilistic forecasting)**
Gauss-M	Gaussian model with the mean imputation as preprocessing
Gauss-R	Gaussian model with the regression-based imputation as preprocessing
Copula	Copula-based imputation model within universal imputation strategy
DeepAR	Deep learning model that uses intermediate results to impute missing values
QR-R	QR model with the regression-based imputation as preprocessing
QR-C	QR model trained based on the complete dataset

Table 2
RMSE values as a function of the lead time (Case 1, missing rate of 20%). RMSE values are expressed in percentage of normalized capacity.

Lead time (steps)	Persistence	RF-M	RF-R	Copula	FCS	DeepAR	RF-C
1	16.8	17.7	16.1	17.3	15.9	17.0	14.6
2	21.1	20.9	19.8	21.3	19.5	20.6	18.9
3	24.7	23.4	22.5	24.3	22.3	23.3	21.9
6	32.7	28.2	28.0	30.6	27.9	29.3	27.6

Table 3
RMSE for one-step-ahead forecasts (Case 1, last feature missing). RMSE values are expressed in percentage of normalized capacity.

Lead time (steps)	Persistence	RF-M	RF-R	Copula	FCS	DeepAR	Retraining
1	15.8	16.2	15.1	15.9	15.0	15.8	15.3

Let us start by presenting and discussing results for the most severe rate of missingness, of 20%. In practice, this means that 20% of the values are missing at random locations over both the training and testing sets. The point forecasting results in terms of RMSE are collated in Table 2.

Unsurprisingly, the RMSE increases with the lead time, and the forecast quality in the presence of missing values is worse than when there are no missing data. There, missing values have a negative impact at both the model estimation and operational forecasting stages. The persistence method is a competitive benchmark, as it is easy to implement and the resulting forecast quality is difficult to outperform for such short lead times. In parallel, RF-M performs worse than the persistence method for one-step-ahead forecasts, most likely due to errors in imputation introduced by this preprocessing procedure. Given training datasets $\boldsymbol{X}^{tr}$ and $\boldsymbol{Y}^{tr}$, one can estimate a regression model f^P that is equivalent to the reference model, if the imputed datasets are the same as the real complete datasets $\boldsymbol{X}^{tr,P}$ and $\boldsymbol{Y}^{tr,P}$. However, the imputed datasets usually deviate from the real complete datasets. Then the model estimated based on $\boldsymbol{X}^{tr,C}$ and $\boldsymbol{Y}^{tr,C}$, denoted as f^C, is different from f^P. That is, the closer the imputed datasets are to the real complete datasets, the closer f^C is to f^P.

Obviously, RF-R has better performance than RF-M, since regression-based imputation is superior to mean imputation. Besides, at the operational forecasting stage, the input features must still be imputed, which may also accumulate errors. Although DeepAR is free of any preprocessing stage, the imputed values may still deviate from real values, introducing errors to both the model training and forecasting stages. As shown in Table 2, the performance of DeepAR is even worse than the simple benchmark model, i.e., RF-R.

The copula- and FCS-based models fall into the category of a UI approach. Compared to the ITP approach, the UI approach has the advantage that it is free of any preprocessing procedure, which avoids introducing errors aroused by the preprocessing procedure into the forecasting task. The FCS-based model outperforms RF-M and RF-R, while the copula-based model is inferior to them, as revealed in Table 2. Although the copula method can characterize several kinds of distributions, the transform function must be specified, which means that a specific distributional assumption is implied. This may impede the performance of the copula-based model when the distributional assumption cannot fit the underlying distribution well. By contrast, the FCS method is free of such an assumption and therefore outperforms the copula-based model. This suggests that by using a distribution-free imputation method like FCS, the UI approach is superior to the ITP approach.

We also compared our proposed approach to the retraining approach discussed by Tawn et al. (2020) by focusing on a specific missing pattern (i.e., when the last feature is missing). The RMSE values are given in Table 3. It is clear that the performance of the retraining approach is comparable to that of RF-M and FCS, as the retraining

Table 4
CRPS as a function of the lead time (Case 1, missing rate of 20%). CRPS values are expressed in percentage of normalized capacity.

Lead time (steps)	Climatology	Gauss-M	Gauss-R	QR-R	Copula	FCS	DeepAR	QR-C
1	18.6	9.2	7.5	7.8	11.5	6.9	7.8	6.9
2	18.6	11.2	9.9	9.9	14.6	9.1	10.2	9.3
3	18.6	12.7	11.7	11.7	17.0	10.9	12.1	11.2
6	18.6	15.9	15.5	15.4	22.4	14.7	16.5	15.1

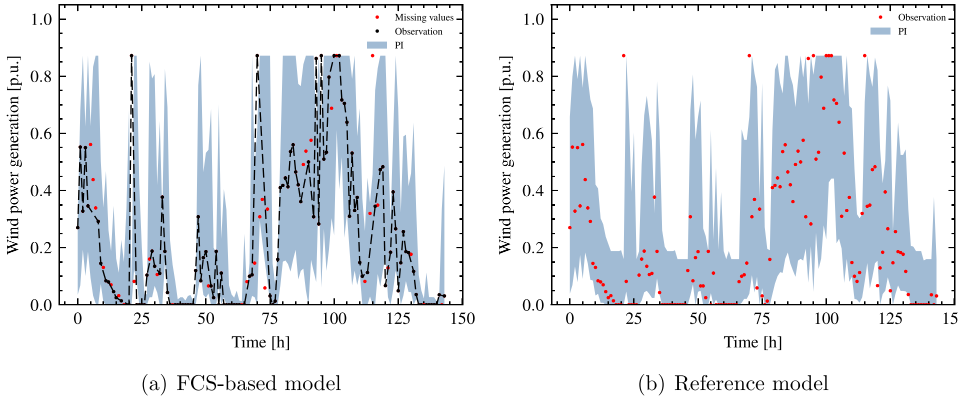

(a) FCS-based model

(b) Reference model

Fig. 8. Illustration of one-step-ahead 90% central prediction intervals over a period of six days, as issued by the FCS-based model (a), and the reference model (b).

approach is free of a preprocessing stage and utilizes a complete set of observations to estimate the parameters. Eventually, the quality of the forecasts is linked to the informative value of the features retained. However, this also implies that a specific model is needed for each missingness pattern. Then, a specific training dataset is required for each pattern, which means that only parts of the data are used to estimate a model. Besides, the retraining approach will suffer from the curse of dimensionality. That is, denoting the dimension of features as d, the retraining approach will independently train 2^d models. While the training time for a set of point forecasting models may be acceptable, the computational costs will steeply increase for probabilistic forecasting cases. In contrast, the proposed UI approach is not only free of any preprocessing stage but also applicable to all missingness patterns once trained.

Next, we move on to the results for probabilistic forecasting. The CRPS values are collated in Table 4. Here, missing values have nearly no influence on the performance of climatology, since climatology characterizes uncertainty based on the empirical distribution of all historical observations. This distribution is not highly modified when a fairly limited number of samples are missing.

Comparing Gauss-M and Gauss-R, we know that a better imputation method is still preferred by the ITP strategy in the context of probabilistic forecasting. Both Gauss-R and QR-R use regression-based imputation as a preprocessing procedure. But they differ in backbone models: Gauss-R relies on the Gaussian distributional assumption, whereas QR-R is distribution-free. Their performance is comparable in this case, and different from the usual situation (i.e., complete datasets) where QR is always superior. Obviously, one needs to estimate the shape parameters of the Gaussian distribution in Gauss-R, but one must estimate the parameters of several quantile functions in QR-R. The parallel estimation of QR-R models may result in more errors in the ultimate estimated distribution. Therefore, the results are governed by both models and the influence of missing values on model estimation. The performance of DeepAR is slightly worse than that of Gauss-R and QR-R, which suggests that handling missing values in forecasting is nontrivial. Values imputed by the intermediate results of the model may also introduce errors at the model estimation stage. The FCS-based model outperforms Gauss-R and QR-R, whereas the performance of the copula-based model is worse than that of Gauss-R and QR-R, which suggests that the distributional assumption may impede the performance of the UI approach. Besides, the performance of the FCS-based model is comparable to that of the reference QR model trained based on the complete dataset, which validates the effectiveness of the FCS-based model.

We present the 90% PIs of six days issued by the FCS-based and reference models in Fig. 8.

Although the FCS-based approach encounters missing values at both the model estimation and operational forecasting stages, its PIs are similar to those of the reference model. Specifically, at some periods, e.g. from 35 h to 45 h, the prediction intervals issued by the FCS-based approach are actually sharper than those of the reference model. A reliability assessment through the use of reliability diagrams is given in Fig. 9(a), while a sharpness assessment is performed by looking at the width of the central prediction intervals (as a function of their nominal coverage rate), and depicted in Fig. 9(b). Models based on an ITP strategy tend to underestimate lower quantiles, while the

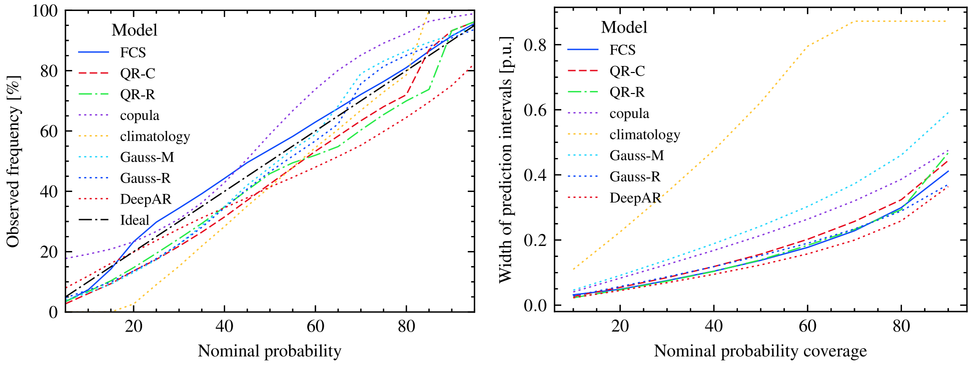

(a) Reliability diagrams

(b) Sharpness diagrams

Fig. 9. Assessment of one-step-ahead probabilistic forecasts for all models for Case 1, based on reliability diagrams (a) and sharpness diagrams (b).

Table 5
The average of absolute values of deviations from perfect reliability in Case 1 (in percentage).

Lead time (steps)	Climatology	Gauss-M	Gauss-R	QR-R	Copula	FCS	DeepAR	QR-C
1	9.20	3.37	3.52	4.81	4.81	2.78	10.57	6.04

Table 6
RMSE values with different lead times in Case 1 on the condition that the missing rate is 10% (percentage of normalized capacity).

Lead time (steps)	Persistence	RF-M	RF-R	Copula	FCS	DeepAR	RF-C
1	15.9	15.9	15.2	16.6	15.1	16.2	14.6
2	20.6	19.7	19.2	20.8	19.1	20.2	18.9
3	24.4	22.5	22.1	24.1	22.0	23.3	21.9
6	32.5	27.9	27.8	30.5	27.8	29.5	27.6

Table 7
CRPS values with different lead times in Case 1 on the condition that the missing rate is 10% (percentage of normalized capacity).

Lead time (steps)	Climatology	Gauss-M	Gauss-R	QR-R	Copula	FCS	DeepAR	QR-C
1	18.6	8.1	7.2	7.4	11.2	6.6	7.4	6.9
2	18.6	10.5	9.6	9.6	14.3	8.9	9.9	9.3
3	18.6	12.1	11.5	11.5	16.9	11.9	9.7	11.2
6	18.6	15.9	15.3	15.3	22.4	14.7	16.6	15.1

reliability of DeepAR and the copula-based model deviates from the ideal case to some extent. The FCS-based model achieves a level of reliability and sharpness that is comparable to the reference model. The average of absolute values of deviations from perfect reliability is shown in Table 5. The deviation of the FCS is even smaller than that of the reference model, which is likely because the FCS is robust to overfitting.

The RMSE and CRPS values, when considering a missing rate of 10%, are collated in Tables 6 and 7, respectively. Compared to the results with a missing rate of 20%, the quality of the forecasts is improved. For point forecasting, the performance of RF-R is comparable to that of FCS, which means that the ITP strategy may be more acceptable when the missing rate is not that high. In the context of probabilistic forecasting, FCS still outperforms other models, which suggests that missing values may pose greater challenges to probabilistic forecasting. Besides, the performance of FCS is even better than that of QR-C, possibly hinting at the fact that FCS is less prone to overfitting.

5.3.2. Case 2

In contrast to the sporadic missingness of Case 1, we here simulate missing values that span over time intervals (hence, referred to as block missingness). Recall that 600 blocks are randomly spread over the whole dataset, with lengths between 5 and 30 time steps. Let us first analyze and discuss the point forecasting results. As a basis, the RMSE values of the points forecasts obtained with the different approaches are listed in Table 8.

The performance of RF-M is comparable to that of RF-R, most likely due to the fact that most samples here are complete. In contrast, the copula-based model performs much worse than both RF-M and RF-R. Indeed, the estimation stage for the copula-based model is based on an expectation–maximization algorithm, which is sensitive to samples whose values are entirely missing. This may suggest that the copula-based model is not applicable to the situation of block missingness. Certainly, the samples whose values are entirely missing contain no information and can be deleted at the model estimation stage. As with Case 1, the performance of DeepAR is worse

Table 8
RMSE values with different lead times in Case 2 (percentage of normalized capacity).

Lead time (steps)	Persistence	RF-M	RF-R	Copula	FCS	DeepAR	RF-C
1	15.8	14.9	14.8	16.4	14.9	15.9	14.6
2	20.9	19.2	19.2	21.1	19.3	21.0	18.9
3	24.8	22.2	22.2	24.3	22.4	24.1	21.9
6	32.9	27.9	27.9	30.6	28.1	30.9	27.6

Table 9
CRPS values with different lead times in Case 2 (percentage of normalized capacity).

Lead time (steps)	Climatology	Gauss-M	Gauss-R	QR-R	Copula	FCS	DeepAR	QR-C
1	18.6	7.0	6.9	7.2	11.2	6.5	7.1	6.9
2	18.6	9.8	9.6	9.7	14.5	9.0	10.2	9.3
3	18.6	11.8	11.8	11.6	17.1	10.9	12.6	11.2
6	18.6	15.7	15.7	15.6	22.4	14.9	17.9	15.1

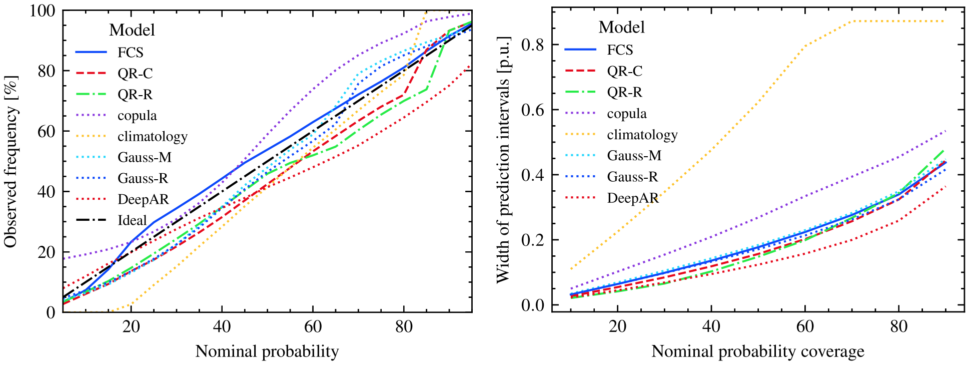

(a) Reliability diagrams

(b) Sharpness diagrams

Fig. 10. Assessment of one-step-ahead probabilistic forecasts for all models for Case 2, based on reliability diagrams (a) and sharpness diagrams (b).

than that of RF-R, which reveals a caveat for the existing DeepAR framework in handling missing values. The performance of the FCS-based approach is comparable to that of RF-M/RF-R. One may then infer that ITP and UI types of strategies perform fairly similarly for point forecasting when experiencing block missingness. However, the picture will look different when extending the study to probabilistic forecasting. To assess the performance of the various approaches for this probabilistic forecasting case, we first look at the CRPS values, which are shown in Table 9.

Unsurprisingly, the performance of Gauss-R is slightly superior to that of Gauss-M. But their difference is smaller than what was observed in Case 1. It could be inferred that it is difficult to handle block missingness via imputation techniques. In the context of block missingness, regression-based imputation will also tend to impute missing values with mean values. Still, the performance of Gauss-R is comparable to that of QR-R. The FCS-based model yields the best performance. Combined with the results of Case 1, this indicates that this approach seems to be superior for different types of missingness, here both sporadic and block missingness. A clear point is that ITP strategies are highly sensitive to samples whose values are entirely missing, since the rationale of ITP strategies is to utilize the observed parts of samples to infer the missing parts. If a sample is completely unobserved, no information could be used for learning and eventually forecasting.

Both reliability and sharpness are evaluated in Fig. 10, for one-step-ahead probabilistic forecasts (with reliability diagrams in Fig. 10(a) and sharpness diagrams in Fig. 10(b). The FCS-based approach achieves acceptable probabilistic calibration, especially in the case of lower and higher quantiles. As summary statistics, the average deviation (in absolute value) for perfect reliability is given in Table 10 for all approaches. There again, one verifies that the FCS-based approach yields the lowest deviation. In parallel, the prediction interval widths for QR, Gaussian-based, and FCS-based approaches are very close, for all nominal coverage rates. The prediction interval width for DeepAR is somewhat smaller, though at the price of poorer probabilistic calibration. This is also reflected by the larger CRPS values for DeepAR, compared to the FCS-based approach.

5.3.3. *Case 3*

In this subsection, we show that forecasting in the presence of missing values can still be improved by utilizing information on nearby sites as auxiliary features (AFs). Besides the input features of the chosen wind farm, we use previous wind power generation values from two

Table 10
Average deviation (in absolute value) from perfect reliability in Case 2 (in percentage).

Lead time (steps)	Climatology	Gauss-M	Gauss-R	QR-R	Copula	FCS	DeepAR	QR-C
1	9.21	4.47	4.27	6.01	8.29	2.69	8.37	6.04

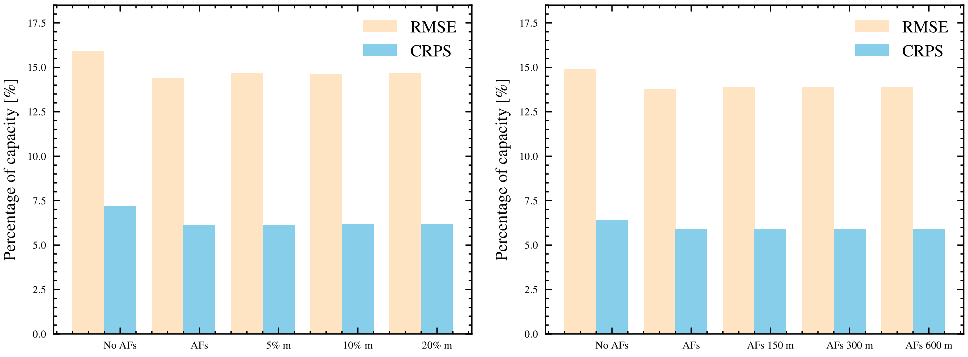

(a) Sporadic missingness case

(b) Block missingness case

Fig. 11. Assessment of one-step-ahead probabilistic forecasts for Case 3, in context of sporadic missingness (a) and block missingness (b).

nearby wind farms as AFs. It is assumed that the missingness of nearby wind farms is different from that of the target wind farm, which is practical since missingness is usually caused by sensor faults or communication errors. We consider both sporadic missingness and block missingness here. Particularly, we concentrate on one-step-ahead forecasts and investigate the impact of different missing rates or missing blocks in AFs. The RMSE values in the context of sporadic missingness are shown in Fig. 11(a) ('AFs *p*% m' means that *p*% of auxiliary features are missing), where we simulate different missing rates at two nearby wind farms and set the missing rate at the target wind farm as 20%.

As expected, the accuracy of point forecasting is improved with the assistance of AFs, which is comparable to RF-C in Table 1. Furthermore, it can be seen that the benefit of AFs is robust, since the performance is relatively consistent as the missing rate of AFs increases. This might be explained by the fact that the key information for forecasting comes from the target wind farm itself. So, it may not make a big difference when a few auxiliary features are missing. The results of probabilistic forecasting are shown in Fig. 11(a), which also suggests that AFs provide extra information and thus contribute to improving probabilistic forecasts. The RMSE and CRPS values in the context of block missingness are presented in Fig. 11(b) ('AFs *c* m' means that there are *c* missing blocks in auxiliary features), where we simulate 600 missing blocks at the target wind farm. It is seen that auxiliary features can still improve the quality of the forecasts in that case.

5.3.4. Training time

We note that by using the FCS method, the proposed UI approach is always superior in the context of probabilistic forecasting. However, it costs much time to perform Gibbs sampling to provide probabilistic forecasting. The computational cost will significantly increase with the dimension of the variable. We present the training time and operational time in Table 11 for illustration. As shown, the training time of FCS is longer than that of QR models, but manageable compared to that of DeepAR. Therefore, we must find computationally efficient methods to implement the proposed approach. As the fully conditional specification method iteratively estimates several conditional distribution models, it is hard to further reduce the training time. But it is feasible to learn the joint probability distribution model directly via a joint modeling approach, which would considerably reduce the training time.

6. Conclusions

It is intuitive to want to consider an impute-then-predict approach to deal with missing values, as existing forecasting methods can be readily used after the (imputing) preprocessing procedure. However, while such a preprocessing procedure at the model estimation stage jointly imputes input features and targets, it only imputes input features at the operational forecasting stage, possibly in a way that is not consistent with the model ultimately used for forecasting. Instead, in this paper, we proposed a "universal imputation" approach, motivated by the problem of wind power forecasting in the presence of missing values. As for many other application areas, it is very common to have missing values in wind power forecasting. Our proposed approach relies on multiple imputation methods, and jointly performs the imputation of missing values of input features and the forecasting of targets. That is, it does not require a preprocessing procedure, while being consistent through the model estimation and operational forecasting stages. Under the assumption that observations are missing at random, parameters can be estimated at the model estimation stage based on observations only. At the operational stage, it treats targets as missing values and iteratively imputes both the missing values of

Table 11
Training time and operational time for one-step probabilistic forecasting in Case 1.

	Gauss-R	QR-R	Copula	FCS	DeepAR
Training time (min)	32	1	9	41	67
Operational time (s)	$\ll 0.01$	$\ll 0.01$	$\ll 0.01$	0.01	0.01

input features and the targets. Particularly, as multiple imputation provides several realizations from the joint distribution of input features and targets, the proposed approach naturally allows for issuing both point and probabilistic forecasts. The case studies based on the WIND Toolkit (over the USA) confirmed the applicability of this approach. Unsurprisingly, forecast quality necessarily decreased as the missing rate of the dataset increased. The results also showed that the FCS-based method performed better than the impute-then-predict approach; it was especially preferred in the probabilistic forecasting case. Furthermore, the results suggested that the FCS-based approach may prevent overfitting to some extent. This also validates the benefits from sharing information and data among wind farms, even in the presence of missing values.

We note that the modeling approach is quite different from the commonly used forecasting approaches in the context of complete datasets. The goal of this paper was not to replace the existing approaches, but rather to offer a complementary tool for use in the presence of missing values. We also expect that there are similar ways to generalize commonly used modeling and forecasting approaches to the case of missing data. The computational costs of the introduced FCS-based approach are high and grow significantly as the dimension increases. Therefore, more efficient methods are still needed. It may be appealing to alternate the FCS method with distribution-free joint modeling imputation approaches. Our proposal is based on the "missing-at-random" assumption and thus avoids modeling the distribution of missingness. The situation where missing observations are not random should be explored in the future. Moreover, emphasis should be placed on relaxing the stationary assumption in order to deal with non-stationary environments, e.g., with online learning.

Declaration of competing interest

The authors declare the following financial interests/personal relationships which may be considered as potential competing interests: Honglin Wen reports fnancial support was provided by China Scholarship Council. Pierre Pinson reports fnancial support was provided by European Union's Horizon 2020. Jie Gu reports fnancial support was provided by Ministry of Science and Technology of the People's Republic of China.

Acknowledgments

This work was performed during a research stay at the Technical University of Denmark. The authors would like to appreciate China Scholarship Council (NO. 202006230261). The research leading to this work is being carried out as a part of the Smart4RES project (European Union's Horizon 2020, No. 864337). The sole responsibility of this publication lies with the authors. The European Union is not responsible for any use that may be made of the information contained therein. Besides, the authors would like to appreciate the reviewers and editors for their constructive suggestions.

References

Benidis, K., Rangapuram, S. S., Flunkert, V., Wang, Y., Maddix, D., Turkmen, C., et al. (2022). Deep learning for time series forecasting: Tutorial and literature survey. *ACM Computing Surveys*, *55*, 1–36.

Cao, W., Wang, D., Li, J., Zhou, H., Li, Y., & Li, L. (2018). BRITS: Bidirectional recurrent imputation for time series. In *Proceedings of the 32nd international conference on neural information processing systems* (pp. 6776–6786).

Cavalcante, L., Bessa, R. J., Reis, M., & Browell, J. (2017). LASSO vector autoregression structures for very short-term wind power forecasting. *Wind Energy*, *20*, 657–675.

Che, Z., Purushotham, S., Cho, K., Sontag, D., & Liu, Y. (2018). Recurrent neural networks for multivariate time series with missing values. *Scientific Reports*, *8*, 1–12.

De Gooijer, J. G., et al. (2017). *Elements of nonlinear time series analysis and forecasting. vol. 37*. Springer.

Dempster, A. P., Laird, N. M., & Rubin, D. B. (1977). Maximum likelihood from incomplete data via the EM algorithm. *Journal of the Royal Statistical Society. Series B. Statistical Methodology*, *39*, 1–22.

The Wind Integration National Dataset (WIND) Toolkit, Draxl, Caroline, Clifton, Andrew, Hodge, Bri-Mathias, & McCaa, Jim (2015). *Applied Energy*, *151*, 355–366.

Gneiting, T., Balabdaoui, F., & Raftery, A. E. (2007). Probabilistic forecasts, calibration and sharpness. *Journal of the Royal Statistical Society, Series B*, *69*, 243–268.

Golyandina, N., & Osipov, E. (2007). The "Caterpillar" -SSA method for analysis of time series with missing values. *Journal of Statistical Planning and Inference*, *137*, 2642–2653.

Goodfellow, I., Bengio, Y., & Courville, A. (2016). *Deep learning*. MIT Press.

Hastie, T., Tibshirani, R., & Friedman, J. (2001). *Springer series in statistics, The elements of statistical learning*. New York, NY, USA: Springer New York Inc..

Hochreiter, S., & Schmidhuber, J. (1997). Long short-term memory. *Neural Computation*, *9*, 1735–1780.

Hong, T., Pinson, P., Fan, S., Zareipour, H., Troccoli, A., & Hyndman, R. J. (2016). Probabilistic energy forecasting: Global energy forecasting competition 2014 and beyond. *International Journal of Forecasting*, *32*, 896–913.

Hong, T., Pinson, P., Wang, Y., Weron, R., Yang, D., & Zareipour, H. (2020). Energy forecasting: A review and outlook. *IEEE Open Access Journal of Power and Energy*, *7*, 376–388.

Hyndman, R. J., & Khandakar, Y. (2008). Automatic time series forecasting: The forecast package for R. *Journal of Statistical Software*, *27*, 1–22.

Januschowski, T., Wang, Y., Torkkola, K., Erkkilä, H., & Gasthaus, J. (2021). Forecasting with trees. *International Journal of Forecasting*, *38*, 1473–1481.

Jones, R. H. (1980). Maximum likelihood fitting of ARMA models to time series with missing observations. *Technometrics*, *22*, 389–395.

Ke, G., Meng, Q., Finley, T., Wang, T., Chen, W., Ma, W., et al. (2017). LightGBM: A highly efficient gradient boosting decision tree. In *Proceedings of the 31st international conference on neural information processing systems* (pp. 3149–3157).

Koenker, R., & Hallock, K. F. (2001). Quantile regression. *Journal of Economic Perspectives*, *15*, 143–156.

Kohn, R., & Ansley, C. F. (1986). Estimation, prediction, and interpolation for ARIMA models with missing data. *Journal of the American Statistical Association*, *81*, 751–761.

Landry, M., Erlinger, T. P., Patschke, D., & Varrichio, C. (2016). Probabilistic gradient boosting machines for GEFCom2014 wind forecasting. *International Journal of Forecasting*, *32*, 1061–1066.

Little, R. J., & Rubin, D. B. (2019). *Statistical analysis with missing data, vol. 793*. John Wiley & Sons.

Liu, T., Wei, H., & Zhang, K. (2018). Wind power prediction with missing data using Gaussian process regression and multiple imputation. *Applied Soft Computing*, *71*, 905–916.

Messner, J. W., & Pinson, P. (2019). Online adaptive lasso estimation in vector autoregressive models for high dimensional wind power forecasting. *International Journal of Forecasting*, *35*, 1485–1498.

Montero-Manso, P., & Hyndman, R. J. (2021). Principles and algorithms for forecasting groups of time series: Locality and globality. *International Journal of Forecasting*, *37*, 1632–1653.

Pinson, P. (2012). Very-short-term probabilistic forecasting of wind power with generalized logit–normal distributions. *Journal of the Royal Statistical Society. Series C. Applied Statistics*, *61*, 555–576.

Pinson, P., McSharry, P., & Madsen, H. (2010). Reliability diagrams for non-parametric density forecasts of continuous variables: Accounting for serial correlation. *Quarterly Journal of the Royal Meteorological Society*, *136*, 77–90.

Salinas, D., Flunkert, V., Gasthaus, J., & Januschowski, T. (2020). DeepAR: Probabilistic forecasting with autoregressive recurrent networks. *International Journal of Forecasting*, *36*, 1181–1191.

Sangnier, M., Fercoq, O., & d'Alché Buc, F. (2016). Joint quantile regression in vector-valued RKHSs. In *Proceedings of the 30th international conference on neural information processing systems* (pp. 3700–3708).

Stekhoven, D. J., & Bühlmann, P. (2012). MissForest–Non-parametric missing value imputation for mixed-type data. *Bioinformatics*, *28*, 112–118.

Stone, C. J. (1991). Asymptotics for doubly flexible logspline response models. *The Annals of Statistics*, *19*, 1832–1854.

Tawn, R., Browell, J., & Dinwoodie, I. (2020). Missing data in wind farm time series: Properties and effect on forecasts. *Electric Power Systems Research*, *189*, Article 106640.

Van Buuren, S. (2018). *Flexible imputation of missing data*. CRC Press.

Van Buuren, S., Brand, J. P., Groothuis-Oudshoorn, C. G., & Rubin, D. B. (2006). Fully conditional specification in multivariate imputation. *Journal of Statistical Computation and Simulation*, *76*, 1049–1064.

Wan, C., Lin, J., Wang, J., Song, Y., & Dong, Z. Y. (2016). Direct quantile regression for nonparametric probabilistic forecasting of wind power generation. *IEEE Transactions on Power Systems*, *32*, 2767–2778.

Wen, H., Pinson, P., Ma, J., Gu, J., & Jin, Z. (2022). Continuous and distribution-free probabilistic wind power forecasting: A conditional normalizing flow approach. *IEEE Transactions on Sustainable Energy*, *13*, 2250–2263.

You, J., Ma, X., Ding, Y., Kochenderfer, M. J., & Leskovec, J. (2020). Handling missing data with graph representation learning. In H. Larochelle, M. Ranzato, R. Hadsell, M. F. Balcan, & H. Lin (Eds.), *Advances in neural information processing systems* (pp. 19075–19087).

Zhao, Y., & Udell, M. (2020). Missing value imputation for mixed data via Gaussian copula. In *Proceedings of the 26th ACM SIGKDD international conference on knowledge discovery & data mining* (pp. 636–646).